Correlations between SO 2 flux, seismicity, and outgassing activity at the open vent of Villarrica volcano, Chile

Correlations between SO_2 flux, seismicity, and outgassing activity at the open vent of Villarrica volcano, Chile

José Luis Palma,[1,2] Eliza S. Calder,[3] Daniel Basualto,[4] Stephen Blake,[1] and David A. Rothery[1]

Received 2 January 2008; revised 23 May 2008; accepted 26 June 2008; published 2 October 2008.

[1] The characteristics of the open vent activity of Villarrica volcano, Chile, were studied in detail by integrating visual observations of the lava lake, analysis of the seismic tremor, and measurements of SO_2 flux. The outgassing activity comprises a persistent gas plume emission from the bottom of the crater as well as frequent explosive events. Three main styles of bubble bursting were identified at the surface of the active lava lake: seething magma, small short-lived lava fountains, and Strombolian explosions. Seething magma consists of continual burst of relatively small bubbles (a few meters in diameter) with varying strength over the entire surface of the lava lake. Small lava fountains, seen as a vigorous extension of seething magma, commonly have durations of 20–120 s and reach 10–40 m high above the lava lake. Correlations between seismicity and visual observations indicate that the seismic tremor is mostly caused by the explosive outgassing activity. Furthermore, for different periods between 2000 and 2006, during which the activity remained comparable, the real-time seismic amplitude measurement system (RSAM) and SO_2 emission rates show a very good correlation. Higher SO_2 emissions appeared to be related to higher levels of the lava lake, stronger bubble bursting activity, and changes in the morphology and texture of the crater floor. Background (low) levels of activity correspond to a lava lake located >80 m below the crater rim, small and/or blocky morphology of the roof, seismic amplitude (RSAM) lower than 25 units, few volcano-tectonic earthquakes, and daily averages of SO_2 emissions lower than 600 Mg/d.

Citation: Palma, J. L., E. S. Calder, D. Basualto, S. Blake, and D. A. Rothery (2008), Correlations between SO_2 flux, seismicity, and outgassing activity at the open vent of Villarrica volcano, Chile, *J. Geophys. Res.*, *113*, B10201, doi:10.1029/2008JB005577.

1. Introduction

[2] Villarrica volcano (39.42°S, 71.93°W, 2847 m above sea level) is the most active volcano in the southern Andes. Like other open vent volcanic systems (e.g., Stromboli [*Ripepe*, 1996; *Bertagnini et al.*, 2003]; Mount Erebus [*Rowe et al.*, 2000; *Aster et al.*, 2003]; and Masaya [*Duffell et al.*, 2003; *Williams-Jones et al.*, 2003]), Villarrica is characterized by persistent degassing and sustained seismicity [*Calder et al.*, 2004]. Since the last eruption in 1984–1985, it has shown persistent gas plume emission and bubble burst activity at the surface of an active lava lake typically located less than 200 m below the crater rim [*Fuentealba et al.*, 2000; *Calder et al.*, 2004]. Open vent volcanoes of low silica composition (e.g., basalts, phonolite) commonly exhibit activity that ranges from sluggish and slowly moving lava lakes, as seen at Erta Ale's summit caldera [*Oppenheimer and Yirgu*, 2002; *Harris et al.*, 2005], to intermittent explosive Strombolian eruptions from multiple vents, as seen at Stromboli volcano [*Ripepe*, 1996; *Ripepe et al.*, 2005; *Patrick et al.*, 2007]. In the former, the formation of a cooled lava crust on top of a convecting degassed magma is a common occurrence, with sporadic bubble bursting also taking place. More explosive activity involves gas slugs rising through a magma-filled conduit and rupturing at the magma free surface [*Ripepe et al.*, 2002; *Aster et al.*, 2003]. Although not sustained for long periods of time, other types of activity such as lava fountains [e.g., *Vergniolle*, 1996; *Andronico et al.*, 2005] and abnormally strong (paroxysmal) explosions [e.g., *Calvari et al.*, 2006] can occur during eruptions or periods of elevated activity. Despite the importance of understanding the characteristics of these eruption styles and the evolution of the activity with time [e.g., *Andronico et al.*, 2005; *Harris and Ripepe*, 2007a], at Villarrica these aspects have not been investigated in detail.

[3] In this study the main characteristics and variations of the continuous Strombolian activity of Villarrica volcano have been identified, and the relationship between seismic-

[1]Department of Earth and Environmental Sciences, Open University, Milton Keynes, UK.
[2]Now at Department of Geological and Mining Engineering and Sciences, Michigan Technological University, Houghton, Michigan, USA.
[3]Department of Geology, State University of New York at Buffalo, Buffalo, New York, USA.
[4]Southern Andes Volcano Observatory, Servicio Nacional de Geología y Minería, Temuco, Chile.

0148-0227/08/2008JB005577$09.00

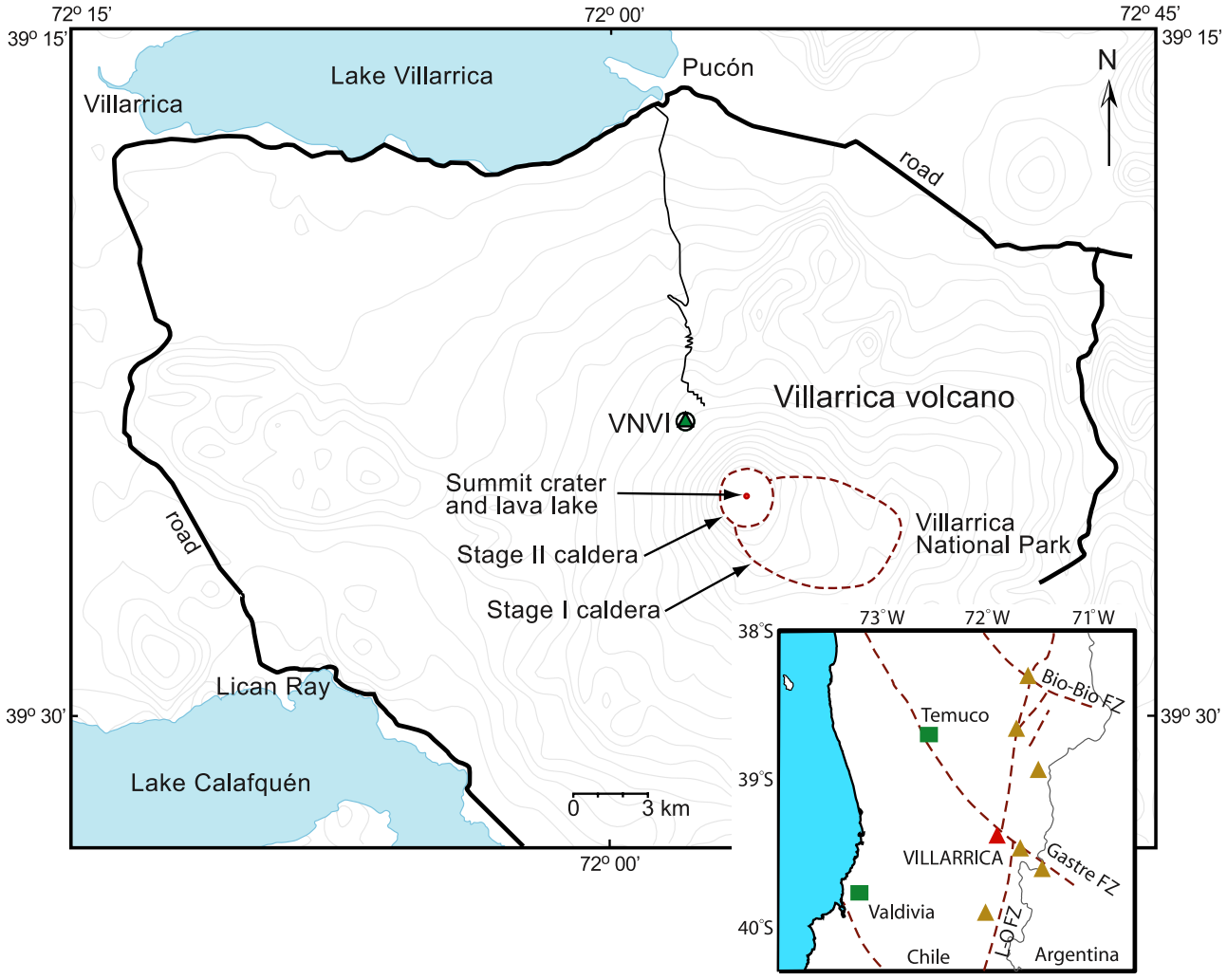

Figure 1. Location of Villarrica Volcano in the southern Andes volcanic zone. The inset map shows some of the major regional tectonic structures (dashed lines, after *Bohm et al.* [2002]): Liquiñe-Ofqui (LOFZ), Gastre and Bio-Bio fault zones. It also shows the cities of Valdivia and Temuco (squares) and the location of other Quaternary volcanoes (triangles). Villarrica volcano is part of a NW–SE volcanic chain that also includes, to the SE, Quetrupillán and Lanín volcanoes. Stage I and stage II calderas of Villarrica were created circa 100 ka (14 ka) and 3.7 ka B.P., respectively [*Moreno et al.*, 1994; *Clavero and Moreno*, 2004]. The summit crater is ~200 m in external diameter with an active lava lake at the bottom. The roads surrounding the volcano on which the ground-based traverses were performed for SO_2 measurements are also shown. VNVI is the seismometer. Contours every 100 m.

ity, degassing, and observed activity at the summit has been established. This was achieved through new measurements of SO_2 flux, seismic data and visual observations pertaining to the period November 2004 to February 2006. Total SO_2 fluxes measured at the summit and around the volcano were correlated with volcanic tremor. Video recordings, photographs, and direct observations of the lava lake activity within the crater allowed us to identify different styles of bubble bursting, and to describe some distinct activity which we consider unique to this particular volcano with its visible active lava lake.

2. Background

[4] Villarrica is an active stratovolcano located in the southern Andes of Chile (33°–46°S) (Figure 1). The snow covered cone is located on the northwest side of an 6.5 × 4.2 km elliptical caldera that was created during the Late Pleistocene (circa 95 ka [*Moreno et al.*, 1994; *Clavero and Moreno*, 2004]). The interior of the crater has a funnel shape and steep inner walls, with an internal diameter of approximately 150 ± 10 m at the crater rim (Figure 2). The predominant composition of lavas and pyroclastic deposits is basaltic to basaltic andesite (50–57 wt % SiO_2) [*Moreno et al.*, 1994; *Witter et al.*, 2004; *Hickey-Vargas et al.*, 2004]. The tectonic setting has been described by *López-Escobar et al.* [1995], *Lavenu and Cembrano* [1999], and *Ortiz et al.* [2003], the geology and composition of the products has been described by *Moreno et al.* [1994], and *Witter et al.* [2004], *Clavero and Moreno* [2004], *Hickey-Vargas et al.* [2004], gas plume composition has been described by *Witter et al.* [2004], *Witter and Calder* [2004], and *Shinohara and*

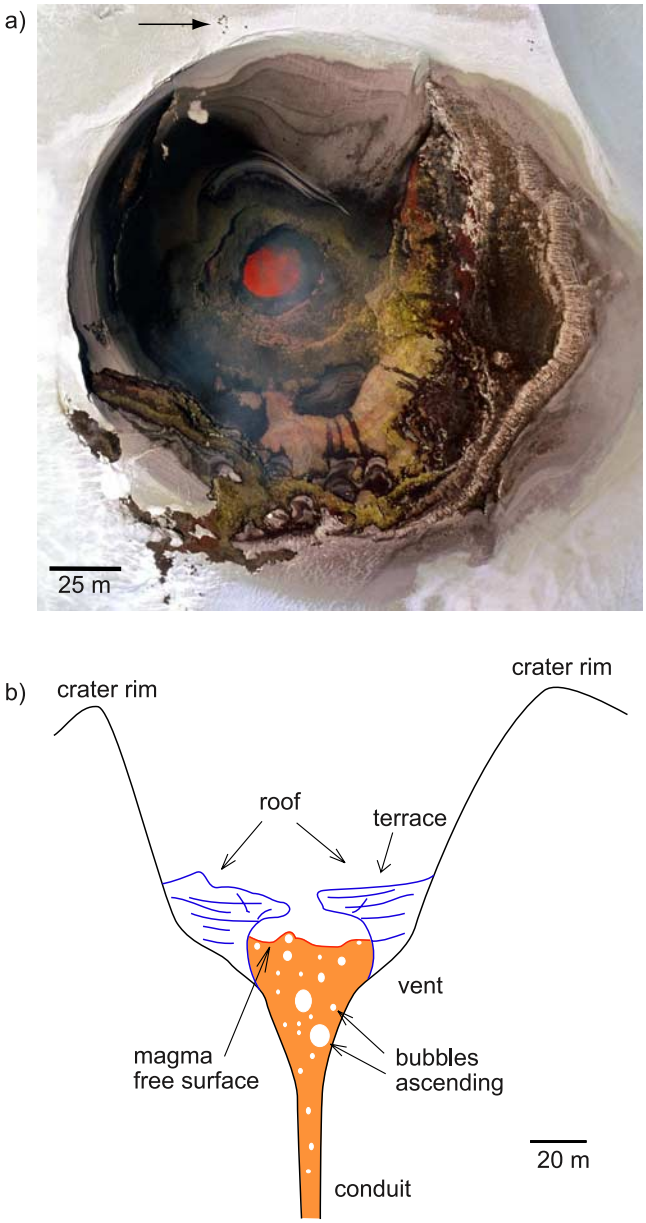

Figure 2. (a) Near-vertical view of the crater of Villarrica volcano in November 2004 (courtesy of C. J. Tanguy). North is toward the top of the photo; the arrow indicates people (black dots) walking on the snow-covered crater rim. The interior of the crater has a diameter of 150 ± 10 m, whereas the outer rim is ~200 m across. (b) Schematic cross section of Villarrica crater. The active lava lake represents the top of the magma column. The spatter roof adheres to the inner crater walls by accumulation of ejected spatter. A terrace (with a relatively flat surface) can be formed by accumulation of tephra during periods of elevated explosive activity.

Witter [2005], and the recent eruptive activity has been described by *Fuentealba et al.* [2000], *Ortiz et al.* [2003], and *Calder et al.* [2004].

[5] Volcanic tremor is one type of seismic signal that characteristically accompanies the activity of open vent volcanoes. It may last for minutes, days, or even months [*McNutt*, 2000; *Zobin*, 2003; *Ripepe*, 1996; *Falsaperla et al.*, 2005]. Several studies have shown a correlation between tremor amplitude and volcanic activity (e.g., Mount Etna [*Falsaperla et al.*, 2005]; Kilauea [*Koyanagi et al.*, 1987]). For instance, the continuous tremor recorded on Etna during the eruption of July–August 2001 showed amplitude and frequency variations that have been linked to the level and style of activity: phreatomagmatic explosions, lava fountains, lava effusion and Strombolian explosions [*Falsaperla et al.*, 2005]. Since the start of the seismic monitoring of Villarrica volcano in 1982, permanent tremor and variable amounts of long-period events have been the dominant seismicity recorded [*Fuentealba and Peña*, 1998]. Other types of signals present in Villarrica seismicity have been classified as explosion events, hybrid signals and volcano-tectonic earthquakes [*Fuentealba and Peña*, 1998; *Calder et al.*, 2004]. The volcano observatory of the southern Andes (OVDAS), of the Chilean geological survey (Servicio Nacional de Geología y Minería), uses a real-time seismic amplitude measurement system (RSAM) [*Endo and Murray*, 1991] as one of the main tools for tracking changes in the volcanic activity at Villarrica.

[6] Measurements of SO_2 concentrations using correlation spectroscopy have proved to be a valuable tool in volcano monitoring, and in the investigation of the dynamics of magma degassing [*Stoiber et al.*, 1983; *Fischer et al.*, 2002; *Young et al.*, 2003]. At Villarrica, there are only a few periods with SO_2 flux measurements. They were mostly carried out by *Witter et al.* [2004] during early 2000 and 2001 to constrain the total gas emission and analyze the dynamics of degassing within the system. Other measurements have been also carried out by OVDAS as part of their monitoring program. Daily averages of SO_2 flux typically revealed moderate emissions ~100–700 Mg/d. Combining SO_2 emission rates with measurements of sulphur and other gas species within the gas plume (as molar ratios) and glass inclusions, *Witter et al.* [2004] and *Shinohara and Witter* [2005] showed that (1) magma ascending to the surface is almost completely degassed, (2) the relative abundance of gas species in the gas plume remains constant during spattering of lava at the vent, which implies that bubbles bursting at the lava lake are in equilibrium with the magma, and (3) on average, ~2.2 m^3/s of magma is degassed. They concluded that convection within the conduit is the most appropriate model of degassing for Villarrica volcano.

[7] In this paper we make a distinction between the terms magma degassing and outgassing. We recognize three main processes responsible for the transfer of magmatic gas from deep magma chambers to the atmosphere: exsolution of gas from the melt, gas segregation and outgassing. Gas exsolution involves bubble nucleation and bubble growth by diffusion of gas into it [*Sparks*, 2003]. Once the gas has been separated from the melt and formed bubbles of sufficiently large size, it migrates upward through a magma-filled plumbing system in the process that is commonly termed "gas segregation." Continuous bubble growth by decompression, gas diffusion, and coalescence occurs during this stage. "Degassing" is a general term often implying any or all of these processes [e.g., *Sparks*, 2003]. The term "outgassing" has been previously used by *Gerlach* [1986], *Ryan* [1995], *Adams et al.* [2006], and *Lautze and Houghton* [2007], among others, to describe the escape of gas from magma. However, despite a consensus on the main

idea, a clear definition has not been provided. Accordingly, magma outgassing is here defined as the escape of gas from the magma either directly to the atmosphere, or to the permeable country rock or hydrothermal system surrounding a magma body. Gas may escape as a segregate gas phase or by diffusion of gas from the edge of the magma body. For instance, gas may escape to the atmosphere by gas diffusion at the surface of a magma column. Hence, outgassing activity includes all the processes of bubble bursting, nonexplosive gas emission, and sustained explosion by which gas escapes to the atmosphere.

3. Recent Activity of Villarrica Volcano

3.1. Background Activity

[8] Since the eruption of 1984–1985, continuous shallow magmatic activity has been seen inside the crater at the summit of the volcano. These observations account for persistent outgassing that involve mild Strombolian activity taking place at the surface of a highly dynamic lava lake, which represents the top of the magma column within the main conduit. Inside the main crater, the lava lake is commonly located at depths ranging from >150 to about 50 m below the summit. Because of the changing morphology of the crater floor, the lava lake is not always visible from the crater rim (Figure 2). Descriptions of the activity at the lava lake by *Fuentealba et al.* [2000] and *Calder et al.* [2004] mention the rapid crusting over of a relatively tranquil lava surface as well as vigorous ~5–30 m high fountaining.

[9] Within this scenario of volcanic activity, background (low to moderate) levels of activity are commonly characterized by the surface of the lava lake being located more than 90 m below the crater rim. Gentle rollover with brief moments of quiescence of the lava lake (as observed by *Calder et al.* [2004]) is likely to mark the lowest strength in activity of the visible lava lake. Strombolian explosions rarely reach 100 m above the lava free surface. In addition, during low levels of activity the tremor amplitude rarely reaches values above 20 RSAM units (persisting for more than 1 day), and the seismicity lacks considerable amounts of volcano tectonic-type earthquakes.

[10] Although these characteristics constrain the predominant volcanic activity observed since 1985, Villarrica volcano displays continuous variations in seismicity, activity observed at the crater, and amount and style of outgassing.

3.2. The 1999 and 2000 Crisis

[11] Three different episodes of high activity have been observed recently: in 1999, 2000, and 2005. These periods developed with abnormal types of observed and seismic activity but did not culminate in eruptions. The first two are documented by *Calder et al.* [2004] and *Ortiz et al.* [2003], respectively, whereas the activity exhibited in 2005 is described in this paper (section 5).

[12] Between August and December 1999, Villarrica showed a significant increase in seismic activity, a rise in the level of the lava lake, several large but discrete explosions, and morphological changes of the crater floor [*Calder et al.*, 2004]. Several episodes of sudden increase in seismic amplitude (twofold or threefold) lasting for several hours occurred in August, November and December. As a result of the explosive activity, scoria bombs up to 50 cm in diameter were found on the crater rim and tephra fall deposits extended up to 5 km from the vent [*Calder et al.*, 2004].

[13] During September 2000, several tectonic earthquakes occurred in the region, including a magnitude 3.8 earthquake that took place less than 70 km from the volcano on 20 September. Subsequently, the tremor spectrum exhibited a frequency shift of its dominant peak from 1 to 2 Hz [*Ortiz et al.*, 2003]. This seismic activity was associated with a sudden decrease in the fumarolic activity observed at the crater, and an apparent crusting over of the lava lake which concealed the nature of magmatic activity. Reestablishment of the activity at the crater was accompanied by pahoehoe flows on the crater floor and the construction of a spatter cone (end of October to beginning of November). During October and November 2000 the seismicity showed peaks at higher frequencies (up to 5 Hz), returning to normal at the beginning of 2001.

3.3. Morphology of the Crater Floor: The Spatter Roof

[14] Cooling at the surface of the lava lake creates partly solidified patches of crust that stay afloat temporarily on the lava surface. At Villarrica, slowly moving crust plates, as seen at Erta Ale [e.g., *Oppenheimer and Yirgu*, 2002; *Harris et al.*, 2005], are not observed. Instead, continually ejected spatter adheres to the inner walls of the vent and forms a spatter roof that grows by accretion and agglutination of the pyroclastic material (Figures 2 and 3a). The spatter roof can partly or completely conceal the activity of the lava lake. The location of this roof also effectively defines the depth of the observable crater floor. The roof is commonly unstable and experiences frequent collapses depending on the intensity of the lava lake activity underneath; when the explosive activity increases, the roof thickens by accumulation of material on its upper surface, eventually creating terraces (relatively flat surfaces, Figure 3b), or even forming a small scoria cone (Figure 3c). The collapsing of the roof or terraces may occur mainly due to the increasing overburden, but also by thermal erosion of its lower surface by the hot magma. Terraces can display concentric fractures which subsequently accommodate collapses. In turn, the outer concentric fracture observed on 16 January (Figure 3b) was the site of a small collapse that occurred within 2 days after the photograph was taken (16–18 January 2005). On 26 January 2005, another small collapse was witnessed by mountain guides. This time, pyroclastic material that had accumulated around an elongated aperture in the spatter roof, not more than 10 m wide, collapsed and left an almost circular opening about 25 m in diameter. When the magma column withdraws and the free surface height lowers, the unstable roof usually collapses often within a time span of hours.

4. Observed Outgassing Styles

4.1. Continuous Outgassing

[15] As mentioned earlier, Villarrica volcano is characterized by the continuous emission of a gas plume from the summit. This ''passive'' gas release is the background outgassing activity observed at the crater. It has persisted since the end of the last eruption in 1985, although a gas

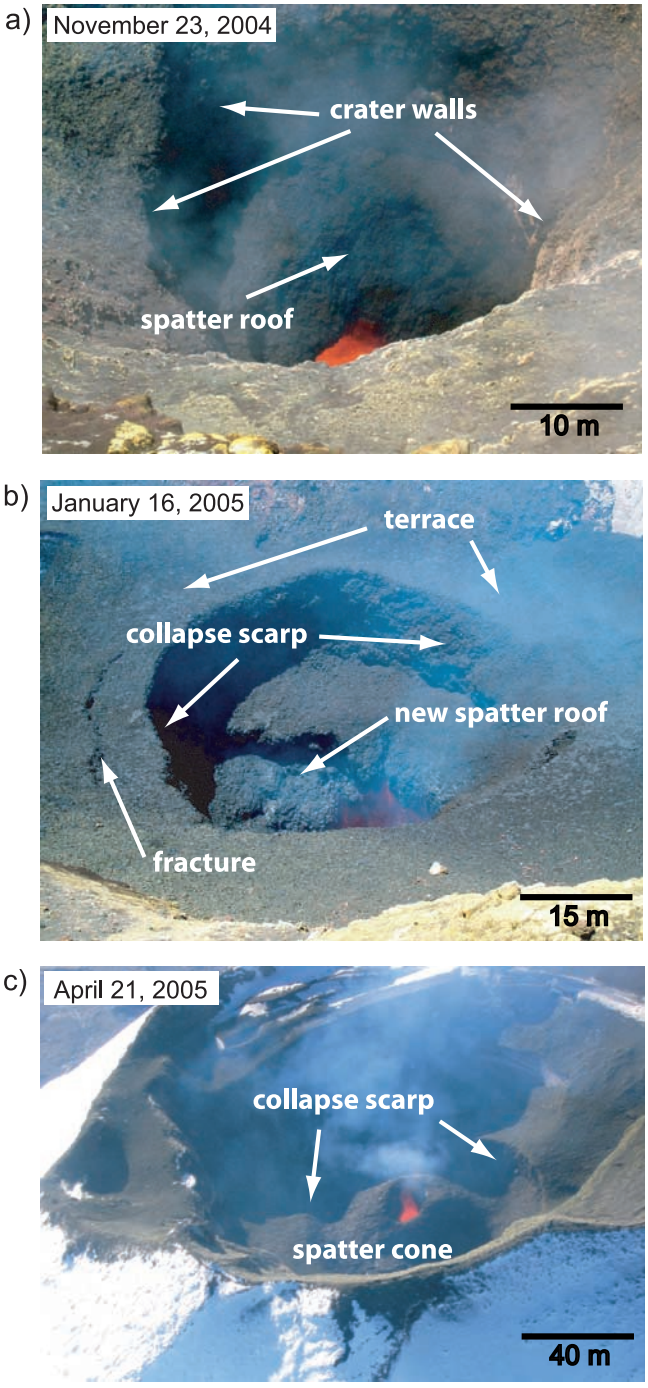

Figure 3. Sequence of photographs that shows the morphological evolution of the vent during the period November 2004 to April 2005: spatter roof and terraces on the crater floor (a) at the end of November 2004, (b) middle of January 2005, and (c) end of April 2005. The position of the roof was approximately 90, 50, and 30 m below the crater rim, respectively. The roof adheres to the walls of the crater above the lava free surface. In Figure 3b a set of three terraces with concentric fractures can be seen; the outer fracture was the site of a small collapse within the next 2 days. Scales are approximate.

plume has been observed recurrently since the end of the 19th century [*Casertano*, 1963].

[16] Direct visual observations from the crater rim along with measurements of SO_2 path length concentrations evidence variations in the emissions from the bottom of the crater. Rough estimations indicate that fluctuations in the gas flux exceed 50% of total emissions. Several factors can contribute to these variations, such as the accumulation of gas inside the lava lake–spatter roof cavity, and the sudden release of higher amounts of gas through explosive activity (in which the gas is vented at higher speeds). Thus, small gas puffs can be seen rising with irregular periodicity from the crater floor. Wind entering the crater intensifies the gas circulation and contributes to further variations in the gas fluxes observed outside the crater. For example, *Bluth et al.* [2007] showed measurements of SO_2 fluxes of the gas plume of Villarrica volcano, up to 3500 m away from the crater, with fluctuations that ranged over a factor of three (between 197 and 640 Mg/d [see *Bluth et al.*, 2007, Figure 2]).

4.2. Bubble Burst Activity

[17] Mild Strombolian explosions are, perhaps, the most common explosive activity observed at the crater. However, five distinct types of bubble burst have been observed during periods with different levels of activity (see Animations S1–S3 in the auxiliary material).[1] Here, the term "bubble bursting" refers to the processes involved in gas bubble rupture at the magma free surface, fragmentation, and subsequent ejection of pyroclastic material. The activity observed includes the following:

4.2.1. Seething Magma

[18] This distinctive bubble bursting, style is distinguishable only when the lava free surface is visible. The activity at the surface of the lava lake resembles the dynamics of boiling water, as medium-sized bubbles (~0.5–2 m in diameter) burst continuously across the magma free surface (Figure 4). Bubbles can be seen to rupture at the same location within the space of a few seconds. This style of activity induces the magma surface to experience continuous wave-like undulations. The vigor of seething magma is variable: on the lower end only a few bubble bursts occur per minute and gentle rollover of the magma surface can be easily identified; at the more vigorous end of the spectrum, there are single bubble bursts almost every second ejecting pyroclasts more than 5 m above the lava lake.

4.2.2. Small Lava Fountains

[19] Fountains of lava occur through a relatively wide roof opening. Compared to the more classic hawaiian style of activity observed at Kilauea volcano [e.g., *Parfitt*, 2004], in which fountains reach tens to a few hundred meters high, these lava fountains are very small and sustained only briefly (Figure 5). They normally last between 20 s and 2 min and reach 10 to 40 m high. To some extent, a small lava fountain resembles a very strong variety of seething magma, with a much greater concentration of bubbles continuously reaching the surface. Although difficult to quantify, it is apparent that most of the pyroclastic material is centimeter-to-decimeter-sized clots of magma. Small lava

[1] Auxiliary materials are available in the HTML. doi:10.1029/2008JB005577.

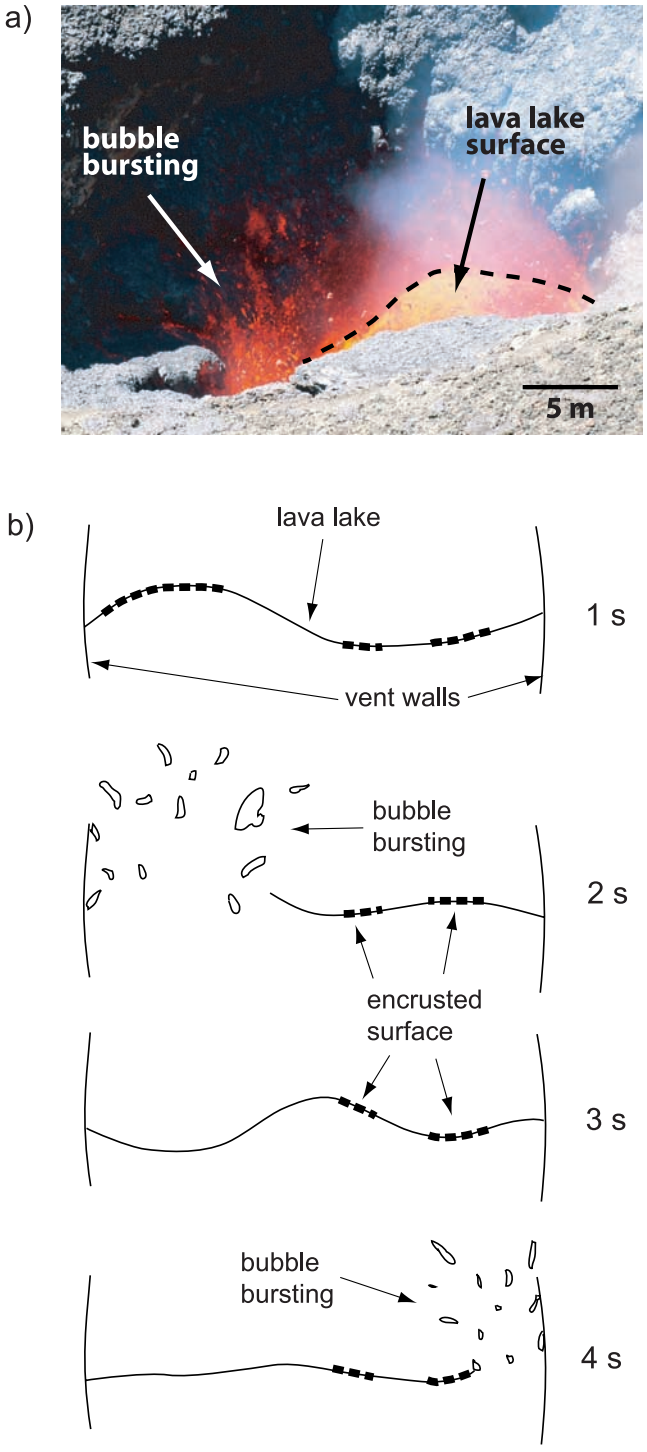

Figure 4. Seething magma bursting style. (a) Photograph of the orifice in the spatter roof that shows part of the lava lake's free surface with a bubble bursting on one side. The dashed black line indicates the margin of the lake. The scale is approximate. (b) Schematic of the seething magma activity, in which undulations occur in a partly encrusted lava lake (thick dash line) because of the bubbles that constantly reach the surface. In this case, two bubble bursts occur in a time frame of 4 s.

fountains are less common than both seething magma and Strombolian explosions.

4.2.3. Strombolian Explosions

[20] This type of bubble bursting, named after the activity at Stromboli volcano, has been described as mild explosions that occur from the rise and rupture of large gas bubbles or slugs at the top of the magma column [*Vergniolle and Mangan*, 2000; *Parfitt*, 2004]. The magnitude and frequency of Strombolian explosions at Villarrica volcano are both variable. Strong explosions ejecting pyroclastic material over 100 m above the vent are mostly seen when the general level of both observed and seismic activity is high, whereas during periods of reduced activity, when the level of magma is low within the crater, it is very rare to see such explosions. The duration of an explosion ranges from a fraction of a second, involving a single strong burst, to more than 15 s when the explosion is composed of rapid sequences of pyroclastic ejections. Because of the morphology of the vent, some explosions do not exhibit pyroclastic ejection through the orifice in the spatter roof, but a sudden and relatively rapid gas emanation that ascends as a distinctive thermal plume. Sometimes, when no spatter is emitted, the spurt of gas is the only evidence of explosions or a strong bubble burst. Strombolian explosions observed

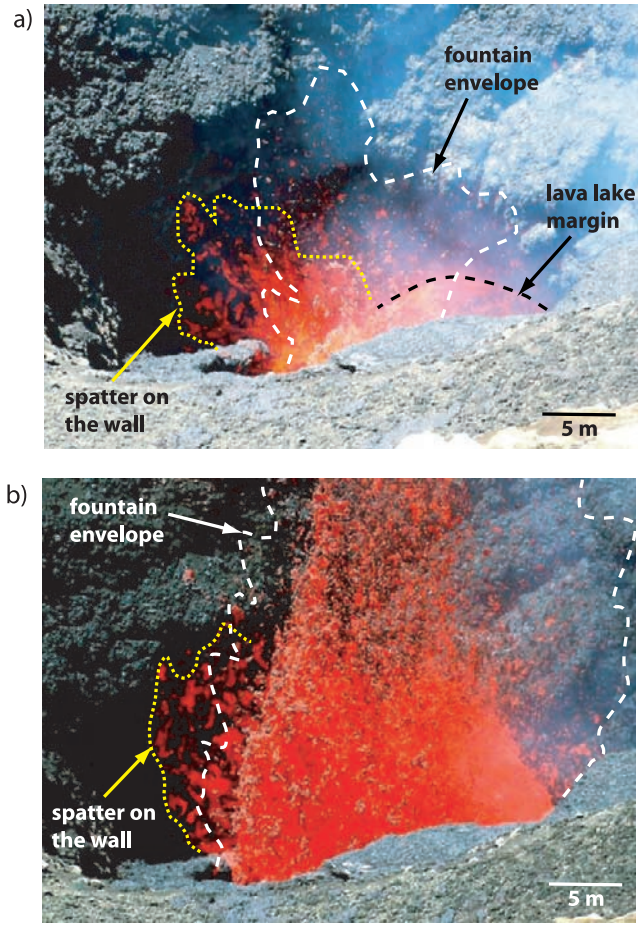

Figure 5. Photographs of the small lava fountain activity. (a) The beginning of the fountain displays a few bubbles bursting simultaneously. (b) Six seconds later, the fountain reaches more than 25 m high. Scales are approximate.

Table 1. Summary of Visual Observations and Seismicity During November 2004 to April 2005

Date	Visual Observations	Seismicity[a]
9–17 Nov	lava lake >100 m below crater rim; not visible; ejected spatter rarely reached more than 20 m above the crater floor	RSAM 10–20 units (average 15)
23 Nov	new spatter agglutinated to the inner wall of the vent	slowly increasing RSAM; up to 20 units
12–19 Dec	explosions send pyroclasts onto the crater rim (>100 m above the lava lake)	RSAM over 20 units and increasing; banded tremor appears interlaced with pulsating tremor
3–12 Jan	apparent increase in frequency of explosions ejecting material out of the vent	highly variable RSAM: 20–35 units and up to 40 on 8 and 9 January
14–18 Jan	spatter roof ~40 m higher than in November; terrace built up with pyroclastic material falling on top of the roof; evidence of partial concentric collapses of the roof around the vent	rapid increase in seismic amplitude: RSAM up to 50 units; seismic signal shows high frequency
21–26 Jan	new accumulation of spatter at the interior of the central opening; big explosions sending bombs above crater rim; partial concentric collapses	RSAM 20–35 units
Feb	morphology of the spatter roof is more stable; explosive activity similar to January; by the end of February, increase in accumulation of pyroclastic material around the vent is evident.	average RSAM ~25 by the middle of February but decreases to 15–22 toward the end of the month
5–11 Mar	pyroclastic material accumulating on the NE–E side of the vent; two holes in the spatter roof	RSAM shows positive trend, recovering values >20 units (on average)
24–30 Mar	opening in the roof has consolidated into one small (~5 m) circular hole; pyroclasts ejected >100 m above the crater rim	RSAM more stable at 20–27 units on average; increasing amounts of VT earthquakes
Apr	a spatter cone is developed on top of the roof with a hole <15 m in diameter; explosions send bombs >150 m above the crater rim; spatter appears around the vent on 19–20 of April	average RSAM stable at 20–30 units; amount of VT earthquakes well above background (36 in the whole month)

[a]RSAM calculated over a time window of 10 min.

at Villarrica are similar to Stromboli type 1 eruptions described by *Patrick et al.* [2007], essentially by virtue of the dominance of coarse particles and lack of a dense ash plume. There have been observations of atypical explosions at Villarrica that are accompanied by a brownish ash plume. They are associated with partial collapses of the spatter roof or avalanches from the inner crater walls, which is concurrent with the idea of backfilling of loose material for the type 2 eruptions at Stromboli [*Patrick et al.*, 2007].

4.2.4. Gas Jetting

[21] Gas jets are strong exhalations of gas and relatively fine (ash-lapilli size) pyroclastic material. Their durations are normally longer than that of Strombolian explosions. None of them have been observed directly generated from the lava lake surface, but instead they originate through an opening in the spatter roof or spatter cone. If the hole in the roof is small, relative to the surface area of the lava lake underneath, it is likely that during an explosion or small lava fountain only the fine fraction of the ejecta vents through the hole, generating the impression of an exhalation of gas with only a small amount of coarse material. There have been observations of near-simultaneous explosions and gas jetting events at two adjacent openings (less than 20 m apart). In that case, the gas jet occurs in the smaller hole (in effect, a blow hole), and commonly lasts as long as the explosion. Gas jet-like activity has also been observed during periods of elevated activity, when a scoria cone has built up on top of the spatter roof, and whose opening is generally narrow. In these instances, the gas jet resembles an energetic narrow fountain whose spatter, ash to bomb in size, can reach a hundred or more meters in height.

4.2.5. Splashing Lava

[22] A fifth type of activity, splashing lava, indirectly related to bubble bursting, has been observed occurring particularly when the spatter roof covers a big part of the lava lake. In this case, the roof prevents the explosions from sending pyroclastic material out of the vent. Often, shortly after an explosion is heard or a gas spurt is observed, a considerable amount of spatter is expelled through the roof orifice. It is characteristically coarse spatter that fragments on exit and accumulates around the vent. We believe that this material is not derived from primary fragmentation of magma during bubble rupturing, but is caused by subsequent splashing of lava associated with waves generated on the lava free surface in the aftermath of an explosion.

[23] These descriptions recognize different mechanisms for the explosive events. While seething magma, Strombolian explosions and small lava fountains represent types of primary bubble bursting activity at the surface of the lava lake, gas jetting appears to result from a combination of bubble burst activity and subsequent interaction with the spatter roof. This interaction modifies the development of the bursting activity and ejection of pyroclastic material as it leaves the vent. This would explain why the size distribution of pyroclasts ejected during gas jetting appears skewed toward smaller fractions compared to that generated as a result of the primary fragmentation. Spatter generated from splashing magma activity is derived directly from the lava lake, although again the fragmentation is not caused by bubble bursting directly.

5. Activity During November 2004 to April 2005

5.1. Chronology

[24] From the end of 2004 and until June 2005, the volcano showed an increase in activity as recorded by seismicity as well as visual observations. A summary of the chronology of the principal events and dates is given in Table 1. The rise in activity levels was accompanied by frequent changes in the morphology of the crater floor (Figure 3). In November 2004 the bottom of the crater was >90 m below the crater rim, from where the lava lake was out of direct view. Spatter from small Strombolian explosions could be seen but rarely reached more than 20 m above the spatter roof. By the end of November, a new small spatter roof had formed at the bottom of the crater (Figure 3a). Subsequently, the activity increased gradually and, by the middle of December, some explosions were

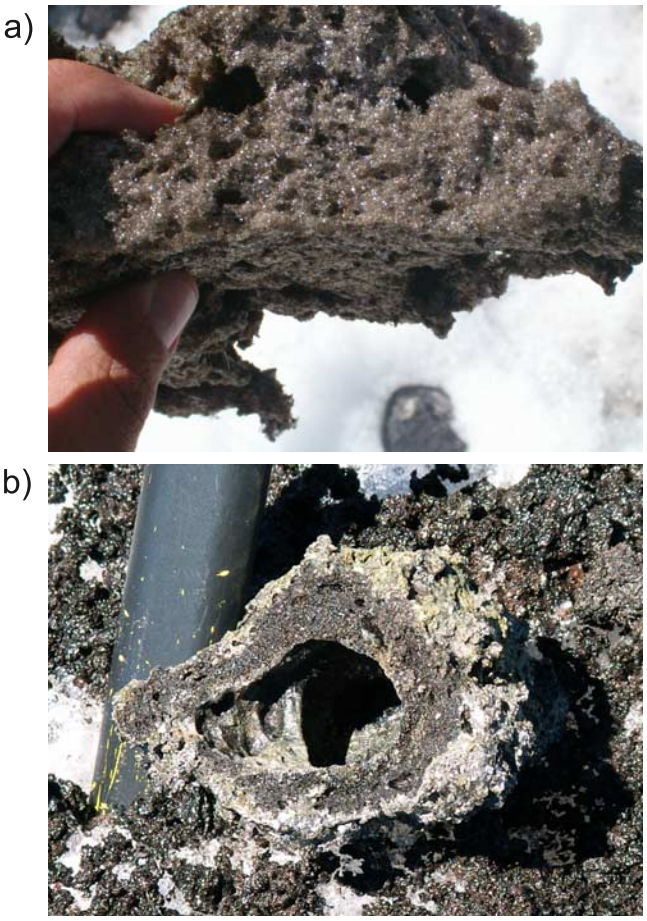

Figure 6. Photographs of two characteristic samples found on the crater rim, generated by explosions that occurred in December 2004 and January 2005. (a) Reticulite scoria that was part of the pyroclastic material thrown >100 m above the crater floor (19 December 2004, 1424 LT); by the next day, not one scoria with that texture remained on the crater rim. (b) Scoria sample showing the wide vesicle-sized distribution commonly found in Villarrica scoria samples (ice axe handle for scale).

sending bombs and spatter up to 100 m above the crater floor. Increasing amounts of new tephra were observed around the vent and also on the crater rim.

[25] During January 2005 the intensity of the Strombolian activity continued to increase, accumulating abundant material on top of the spatter roof and crater walls. Although it was unusual to see large explosions during the time spent at the summit of the volcano (usually between 1.5 and 3.5 h), by the middle of January it was more common to find new pyroclastic material (lapilli-bomb sized) on the northeast side of the crater rim. During this period, the morphology of the crater floor was evolving rapidly and showed evidence of repeated construction and partial collapse cycles. A prominent upper terrace formed only ~50 m below the crater rim, suggesting the rise of the magma free surface. The second half of January was characterized by a rapid increase in the level of activity and, by the end of month, explosions were ejecting centimeter-sized pyroclasts up to ~100 m above the bottom of the crater (~50 m above the crater rim).

[26] There were no further substantial changes until late February and early March when the upper terrace increased in thickness by accumulation of pyroclastic material. By the end of March, a small spatter cone started to grow on top of the roof with an orifice less than 10 m in diameter on its top (Figure 3c). During April the roof morphology kept changing, notably the size of the cone and diameter of its vent. The small vent acted as a nozzle generating narrow, vertically directed jet-like explosions. The most vigorous explosions observed from the crater rim had durations of the order of 3–10 s and ejected bomb-sized pyroclasts at least 150 m above the crater floor. This explosive activity continued through May and explosions throwing material above the crater rim were seen until July. By the end of July to early August the lava roof (and magma free surface) had retracted to about 70 m below the crater rim, which was accompanied by a decline of the activity, marking the end of the 2004–2005 episode.

[27] Pyroclasts derived from explosions exhibit vesicles with a broad size distribution. Two examples of typical pyroclasts found on the crater rim of Villarrica volcano are shown in Figure 6. Reticulite is common among this material (Figure 6a). General textural characteristics of scoria found on the crater rim include high vesicularity (>60% in the most vesicular samples) with vesicle radii up to a few centimeters (Figure 6b), irregular and iridescent surface with adhered Pele's hair, or spatter with cowpat-like form (elongated and flat) in some products of big explosions. Often after an explosion, it is only the more dense material that remains on the crater rim as the highly vesicular ejecta is easily dispersed by the wind. Observations of millimeter to centimeter-sized vesicles in scoria samples, along with observations of the meter-sized bubbles bursting at the lava lake, are an indication of a very broad bubble size distribution in the gas phase reaching the magma free surface.

5.2. Characteristics of the Seismic Tremor

[28] During November 2004 to April 2005, two short-period vertical component seismic stations were operating near the volcano, at 3.7 km (station VNVI) and 19 km (station CVVI) to the NW and W of the crater, respectively (Figure 1). Both are part of the volcano monitoring seismic array operated by the Southern Andes Volcano Observatory (OVDAS-SERNAGEOMIN). In this study, we utilize data from the VNVI station, which is the closest station to the volcano. We do not correct for the frequency response of the seismometer, which is flat above the corner frequency of 1 Hz. This limits the quantitative analysis of frequency peak amplitude and dominance below 1 Hz, but it does not affect the temporal analysis of amplitude and frequency variations.

[29] Tremor at Villarrica contributes more than 90% of the total seismic energy. It is commonly a continuous, irregular and low-amplitude seismic signal. Its waveform generally has a pulsating pattern in which short tremor bursts of higher amplitude occur as often as once per minute (Figure 7). The frequency of occurrence of the higher-amplitude bursts varies with the level of activity (*Calder et al.* [2004] reported 10 events per hour in 1999). Periods of elevated observed volcanic activity have an overall higher occurrence of these events. If viewed as individual discrete events, these higher-amplitude bursts normally last

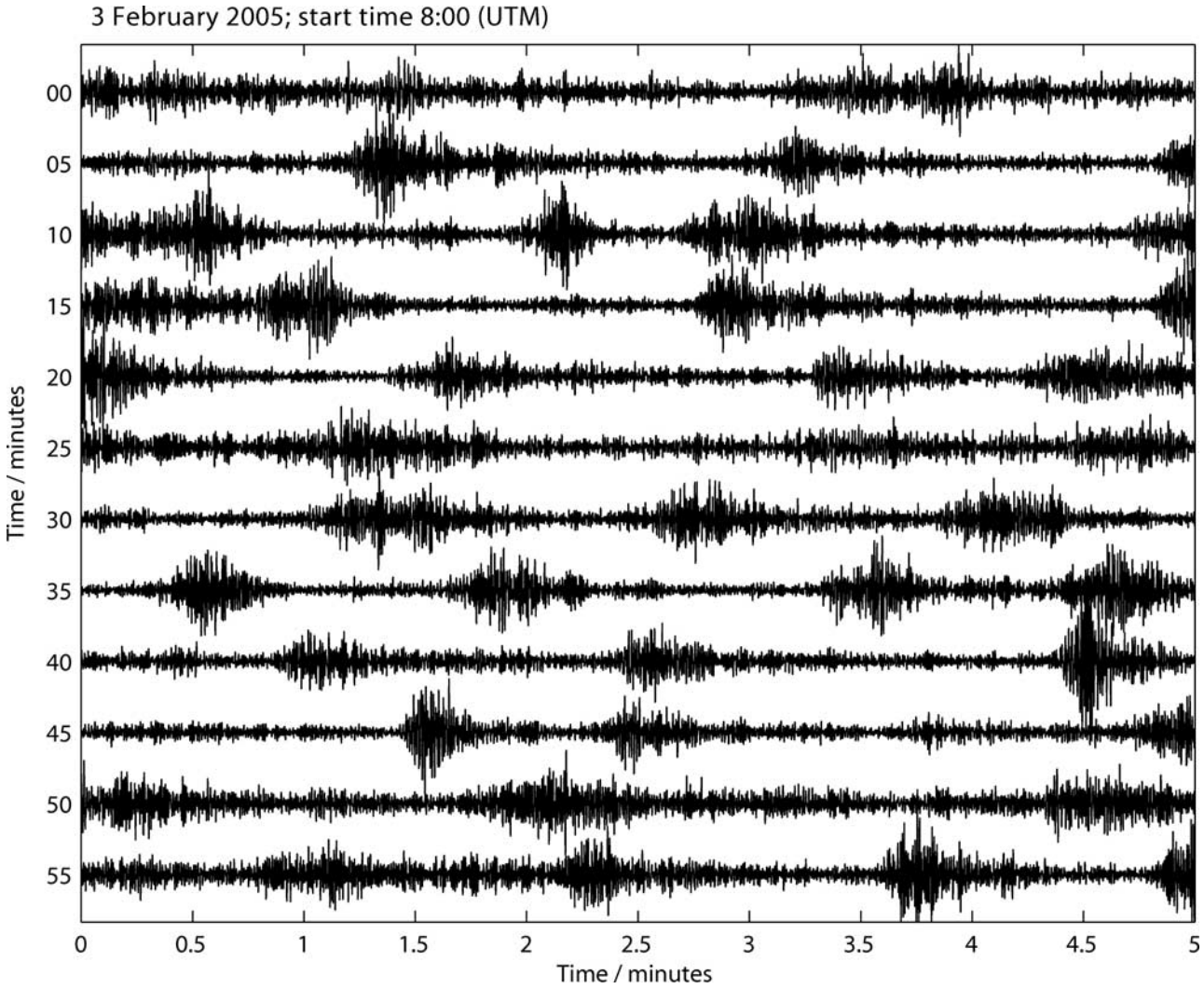

Figure 7. One hour of seismicity from 3 February 2005 beginning at 0500 LT. The vertical axis shows the start of the signal at 5-min increment. Individual bursts have a wide range of amplitudes and durations, as well as emergent starts and ends.

less than 50 s, are generally characterized by emergent starts and ends (gradual increase and decrease in amplitude, respectively), and show a wide range of amplitudes and durations (Figure 7). They have been previously described as low-frequency events generated by Strombolian explosions [*Fuentealba and Peña*, 1998; *Fuentealba et al.*, 2000].

[30] Banded tremor, as described in the literature of Kilauea volcano [*Koyanagi et al.*, 1987], is also characteristic of the seismicity of Villarrica volcano. Such higher-amplitude tremor can last minutes to days, but commonly has a duration of a few hours. Typically, it preserves the spectral features of the lower-amplitude tremor preceding it. Banded tremor repeats during the period of study and has been described during the 1999 crisis [*Calder et al.*, 2004].

[31] One of the main tools employed by the Southern Andes Chilean Volcano Observatory (OVDAS), to routinely monitor the activity of Villarrica volcano, is the amplitude of the seismic signal, which is measured as RSAM units [*Endo and Murray*, 1991]. Changes and trends in seismic amplitude (RSAM) for the period November 2004 to April 2005 correlate well with the volcanic activity described above (Table 1 and Figure 8a). RSAM started increasing in December and continued increasing until the end of January, reaching values of between 40 and 50 RSAM counts. There was a decrease in amplitude at the beginning of February, although remaining higher than 20 counts, and a further sudden decrease that is followed by a slow increase starting the last week of February and reaching values of 30 counts by the middle of March. During the second half of March and April, the RSAM values remained fairly constant between 20 and 30 counts. In general, these variations are manifested by the total range and maximum values of the RSAM amplitude (Figure 8a). In addition to the long monthly trend in seismic amplitude there are some short episodes, normally just a few days, where the overall RSAM amplitude changes abruptly to higher or lower values (e.g., 14–19 and 29–30 January 2005). One of these episodes, at the middle of January, was correlated with increasing gas emissions (section 6.2).

[32] Throughout the analyzed period most of the seismic energy is concentrated within the frequency range 1–7.2 Hz, with the highest peaks commonly between 1 and 2.15 Hz

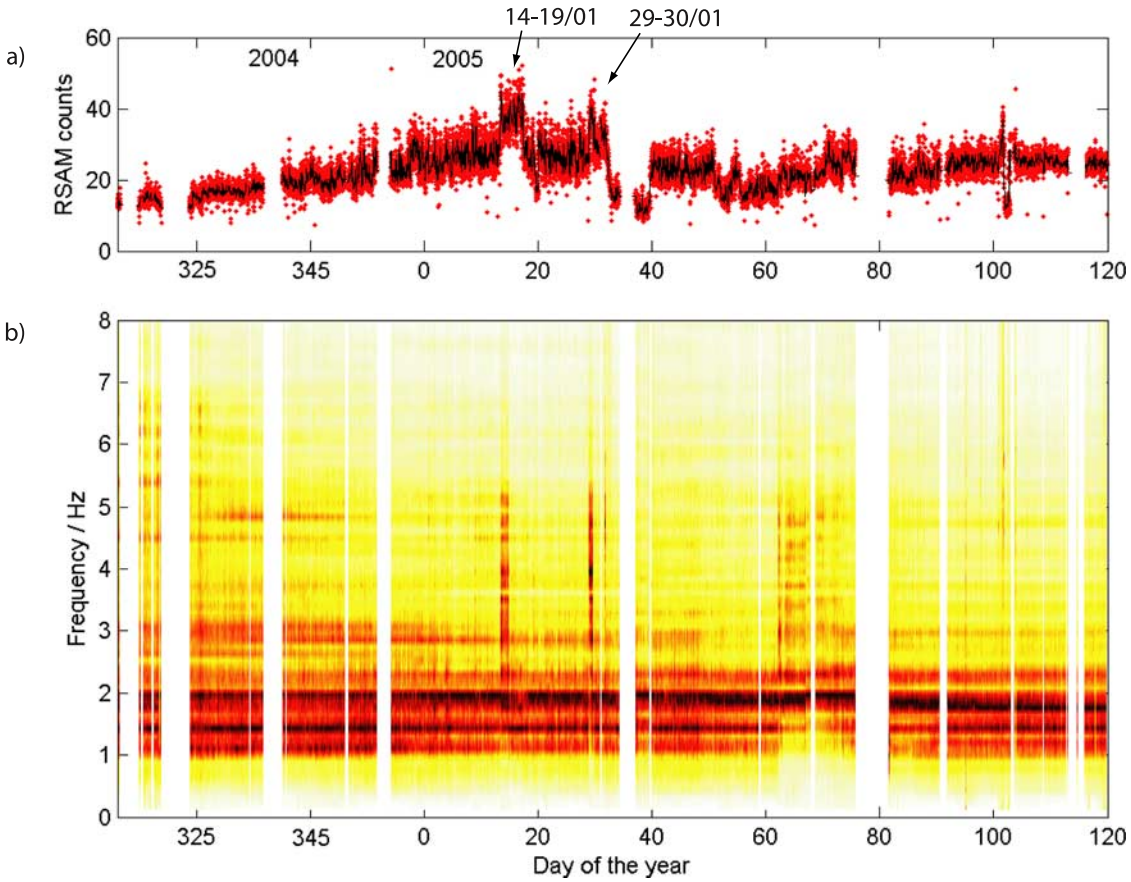

Figure 8. (a) Real-time seismic-amplitude measurements (RSAM) and (b) spectrogram of the tremor for the period November 2004 to April 2005. RSAM is calculated over a moving window of length and step of 10 min. The spectrogram is normalized to the maximum value of the energy for every 10 min window, so it shows the relative changes in frequency distribution and dominant spectral peaks. Empty spaces represent data gaps.

(Figures 8b and 9). Along with the increasing activity from November 2004 to January 2005, the associated tremor displayed gradual variations in the relative amplitude of the dominant peaks in the frequency domain: the amplitude in the frequency band 1.65–2.15 Hz increases whereas in the frequencies bands 1–1.35 and 2.55–7.2 Hz the relative amplitude decreases (Figures 8b and 9). Sharp changes in amplitude within the range 2.55–5.5 Hz, occurring on 14–19 and 29–30 January 2005, strongly contribute to the sudden increases in RSAM values (Figures 8, 9, and 10). These variations last for a few hours or days and do not represent individual transient events. The relationship between these short periods of higher amplitude and the activity observed at the summit of the volcano is not clear. Although environmental effects such as high winds cannot be ruled out, weather reports and observations in the field did not point to any particular meteorological conditions that would coincide with the timing of these variations. Moreover, a closer look at the signal reveals different amplitudes and start times of these peaks at low and high frequencies (Figure 10). The onset of the tremor with highest amplitudes in the band 2.15–7.2 Hz coincides with a decrease in the amplitude of the band 1–2.15 Hz. Only a few hours later, when the amplitude of the relatively high frequency band (2.15–7.2 Hz) is in a waning stage, the low-frequency band (1–2.15 Hz) recovers its previous amplitude (Figure 10). Unfortunately, detailed visual observations of the crater on some of these days (16 and 18 January 2005) were not sufficient to allow the correlation of these variations with the volcanic activity.

[33] During periods of elevated seismic activity, such as in December 2004 and January 2005, the daily RSAM exhibited a broad range of values with a fast increase and subsequent slow fall in amplitude (Figure 11a). These fluctuations had a periodicity of about 1.9 to 5 h, but the most prominent saw-tooth cycles commonly had a duration between 2 and 3.5 h. Seismic traces coincident with high RSAM units evidence a higher frequency and amplitude of the tremor bursts (Figure 11b), although the frequency content of the tremor is similar on both RSAM peaks and RSAM troughs (Figure 11c). During periods where the RSAM was low (<20 units), these features were absent or appeared more erratic and less frequent.

5.3. Correlation Between Outgassing Activity and Tremor Magnitude

[34] Simple experiments were carried out between January and February 2006 in order to correlate the seismic signal with the observed activity at the summit of Villarrica volcano. From the crater rim, we made timed observations

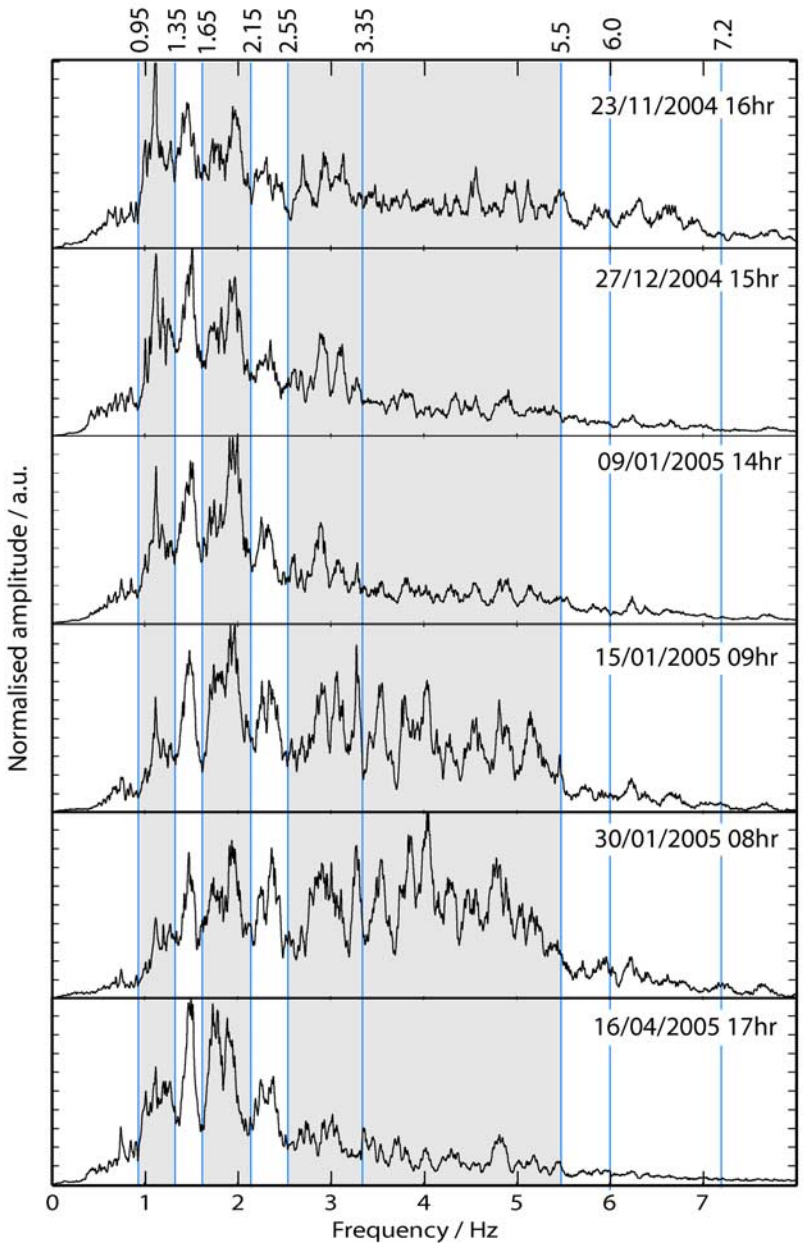

Figure 9. Spectra of six 1 h long seismic signals that show the changes in the amplitude of the predominant peaks between November 2004 and April 2005. Vertical lines divide the spectra at frequencies 0.95, 1.35, 1.65, 2.15, 2.55, 3.35, 5.5, 6, and 7.2 Hz. These lines were chosen in order to highlight the variations in amplitude of particular frequency ranges. Gray areas correspond to frequency bands 0.95–1.35, 1.65–2.15, and 2.55–5.5 Hz.

of the explosions and other outgassing related events (Figure 12). During this period the level of activity was considered low, with the bottom of the crater located more than 80 m below the crater rim. The diameter of the orifice in the roof was no greater than 15 m and so the lava lake was not directly visible. A second small hole was present on the west side of the roof and showed continuous gas emission with only sporadic pyroclastic activity. Owing to morphological restrictions not every bursting event could be observed. In spite of that, the results show a good correlation between the timing of the observed bubble bursts and that of higher-amplitude tremor transients (Figure 12a). Moreover, the frequency content of the seismic signal, evaluated as the relative contribution of bands 0.95–2.15, 2.15–3.35 and 3.35–5.5 Hz, was observed to change slightly with time. This was particularly evident on high-amplitude tremor bursts (Figure 12a). However, despite the apparent higher component of low-frequency energy on tremor peaks, there was no consistent variation in the frequency content of low- and high-amplitude tremor (Figure 12b). This characteristic has been also observed in other periods, such as December 2004 to January 2005. Hence, the higher-amplitude tremor transients are not distinguishable based upon their frequency content alone.

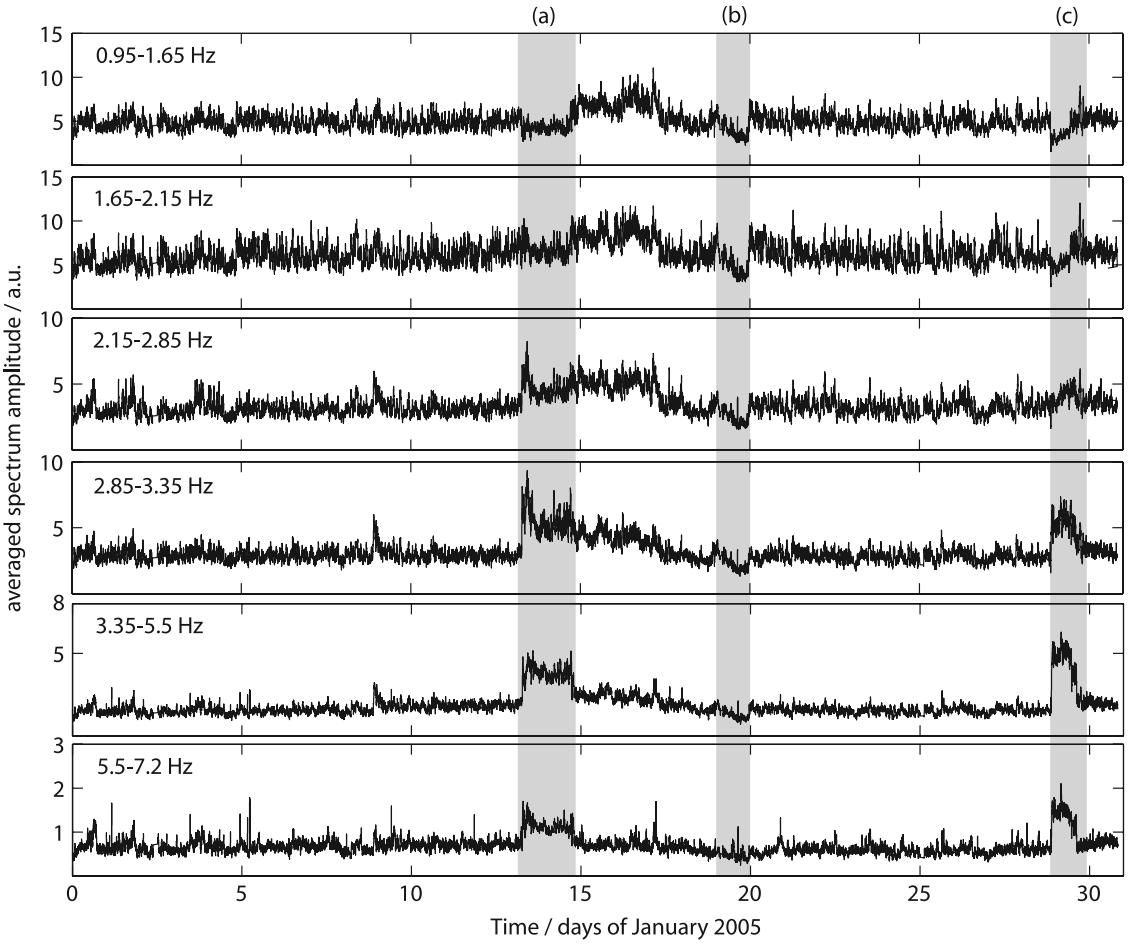

Figure 10. Amplitude variations in the frequency of the tremor during January 2005. Each trace was obtained by calculating the fast Fourier transform (FFT) and averaging the spectral amplitude of a 30 min long window moving with a step of 15 min. Frequency bands were chosen on the basis of the distribution of peaks and troughs in the spectra after inspection of the whole data set. Note the different scales on the vertical axes. Although the amplitudes are in arbitrary units, values between bands can be compared.

5.4. Statistics of the Tremor

[35] In order to assess the fluctuations in amplitude of the seismic tremor, three statistical parameters have been calculated from a high-resolution RSAM of the seismic signal: (1) RSAM mean ($\overline{\text{RSAM}}$), (2) RSAM standard deviation (σ), and (3) rate of high-amplitude tremor burst. Details of the procedure to calculate them can be found in Appendix A. One of the advantages of processing the seismicity on the basis of a high-resolution RSAM time series, obtained from time windows of 10 s duration, is that it allowed the identification and counting of the tremor events. In addition, the RSAM mean and standard deviation yielded information about the difference in amplitude of the background low-amplitude tremor and higher-amplitude events, as well as the occurrence of exceptional bigger events. As shown in the example of Figure 13, all three parameters vary greatly, $\overline{\text{RSAM}}$ from 16 to 36, σ from 4 to more than 8, and events rate from 1 to 2.4 per minute. Also, the combination of their values varies continuously with time. These variations indicate that, unlike the more steady frequency content of the tremor (Figure 11), its amplitude can change considerably over a short time span. Further, the combination of these parameters can describe relevant characteristics of the tremor waveform. For instance, low events rate along with low RSAM mean and high standard deviation (e.g., area a in Figure 13) represent relatively less frequent high-amplitude discrete events with well defined starts and ends (not overlapping with each other). It is noteworthy that if the duration of the window used in the calculations of the statistics is short, one single big event can increase the standard deviation substantially (as observed in area b of Figure 13). The opposite arrangement, with high events rate and very low standard deviation (e.g., area c in Figure 13), represents tremor with a steady envelope in which events of similar amplitude occur more frequently; the amplitude of these events can be determined by the magnitude of the RSAM mean.

[36] Although the overall trend of events per minute might display a rough correlation with the amplitude of the RSAM (e.g., Figure 13), during November 2004 to April 2005 neither the RSAM standard deviation nor the events rate showed a consistent correlation with the RSAM amplitude. An example of this is shown in Figure 14. During the distinct changes in RSAM amplitude in January

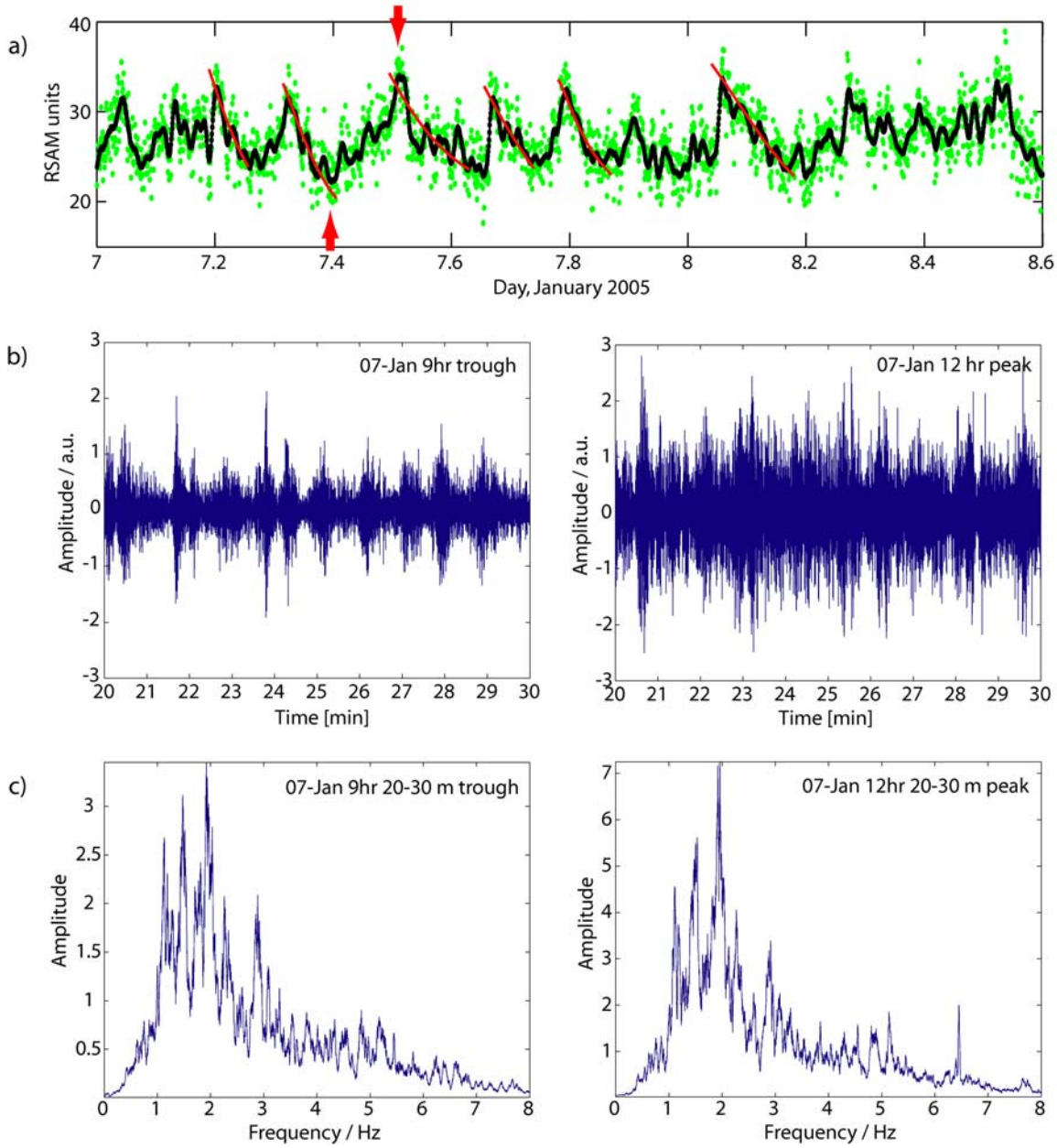

Figure 11. (a) Fluctuation patterns in seismic amplitude (RSAM). This example is from 7 to 8 January 2005. Many of the fluctuations display a serrated shape, with a fast increase in amplitude followed by a slow decrease. (b) Waveform plots of 1 h of seismic signal coincident with an RSAM peak and RSAM trough (indicated with arrows in Figure 11a). (c) Their associated frequency distribution (Fourier transform).

2005, both the standard deviation and the event rate showed patterns different to that of the RSAM mean. Some noteworthy features are those that occurred on the 14–15 and 29–30 January (areas a and c in Figure 14, respectively), in which the events rate per hour increased and subsequently decreased sharply, and correlated with the inverse fluctuations in standard deviation; the RSAM displayed a rather different behavior. In turn, the peaks in RSAM amplitude and standard deviation denote the occurrence of relatively high amplitude tremor events on a time span of a few hours (e.g., 0900–1200 LT 14 January, 1500–1600 LT 30 January). The trough in standard deviation accompanied by higher RSAM denotes banded tremor (e.g., 29–30 January). On 20 January (area b in Figure 14), however, the tremor events rate followed the decrease in RSAM mean amplitude, in the same manner as all frequency bands did (Figure 10), denoting a considerable drop in seismic activity.

[37] Hence, the three statistical parameters presented here yield meaningful information that can be used in the analysis of seismic variations and its relation with volcanic activity.

5.5. Volcano-Tectonic Earthquakes

[38] Volcano-tectonic (VT) earthquakes, also called high-frequency events [*McNutt*, 2000, 2005], are uncommon in

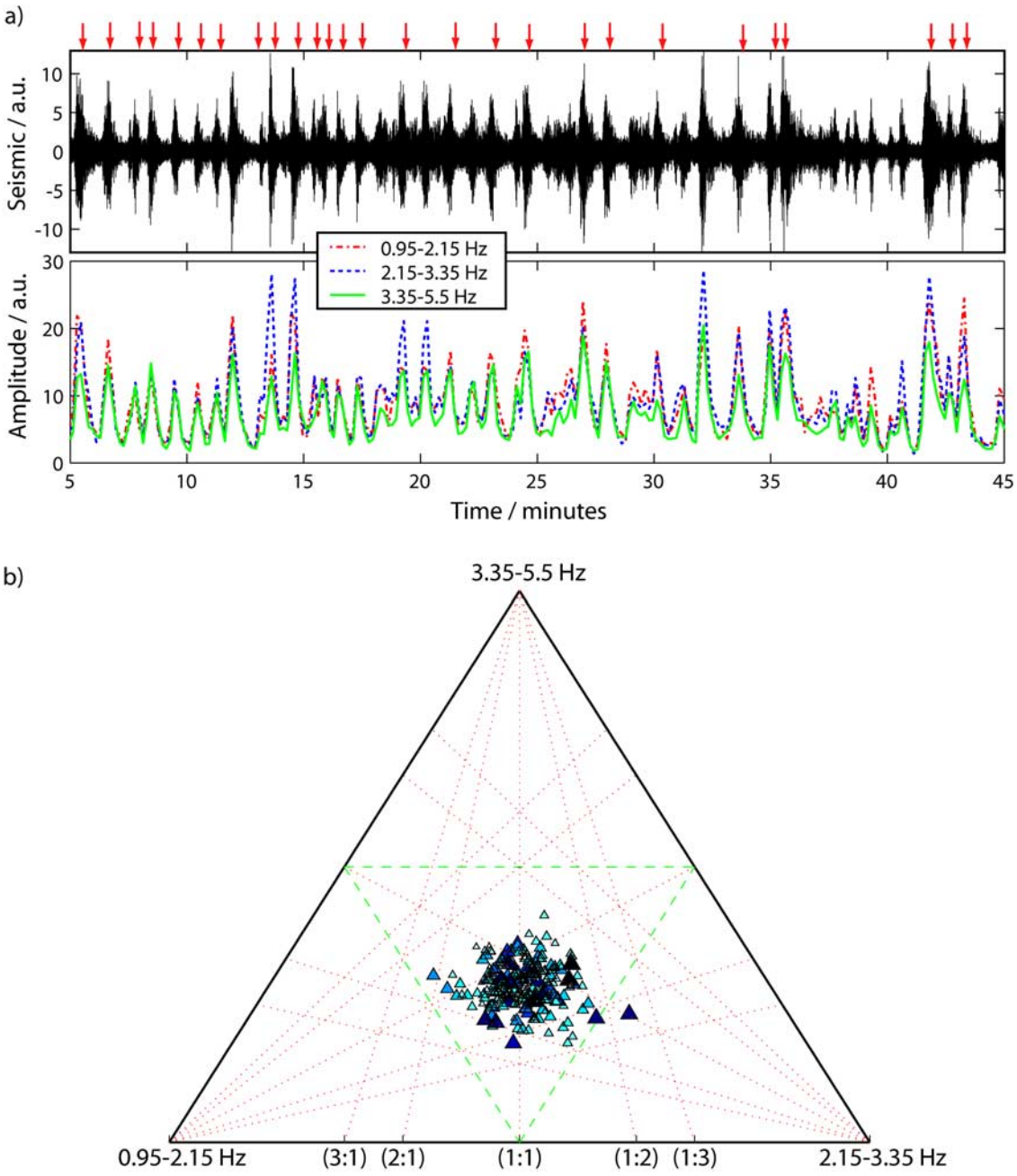

Figure 12. Example of the correlation between visual observations of explosions and seismicity at Villarrica volcano. (a) Seismic tremor and amplitude of three frequency bands are illustrated considering 40 min of data of 17 January 2006. Arrows on top mark the time of explosions observed from the summit of the volcano. The amplitude of the frequencies was calculated with a 15 s long moving window with a step of 10 s. (b) Distribution of the frequency content for the same signal. Higher-amplitude tremor is represented by darker and bigger triangles.

the seismicity of Villarrica volcano. Only a few of these events are reported every month during periods of low (background) activity (between 1 and 3 [*Calder et al.*, 2004]). During the elevated volcanic activity of December 2004 to July 2005, however, as many as 10 and 36 VT earthquakes were identified in March and April, respectively (Table 2). The small number of stations in the local seismic network operating during that time period did not allow the location of these events. Nevertheless, three major VT earthquakes that occurred on 6 April 2005 were clearly recorded by the seismic network located at neighboring active volcanoes (Llaima, Lonquimay and Calbuco volcanoes) as well as in the city of Temuco. Analysis of data from 9 stations located between approximately 4 and 220 km away from the volcano, using the Hypo 71 algorithm under the software SEISAN, allowed the localization of these events within 8 km to the northeast of Villarrica crater. These results support the idea of a change in the stress state

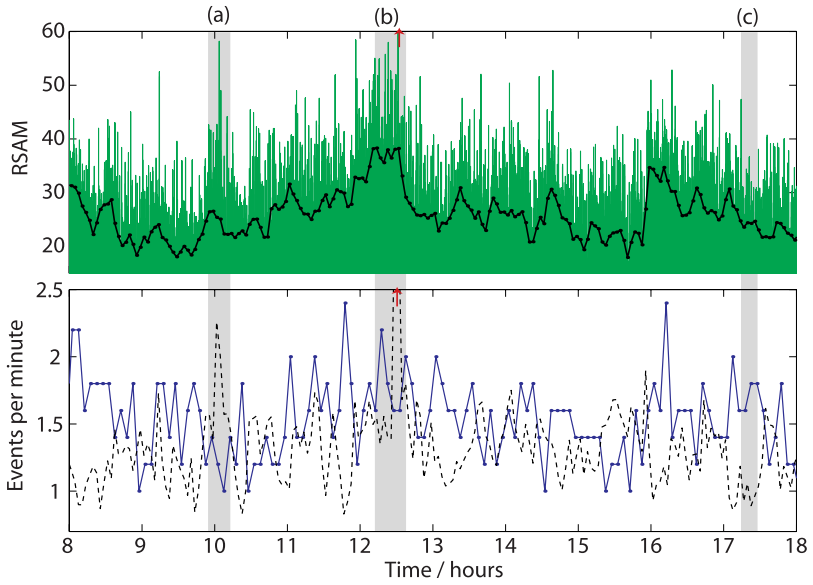

Figure 13. Statistics and event counting of the tremor. (top) A high-resolution RSAM (bars) calculated with a 10 s long window moving with a step of 7.5 s. The continuous line is the average RSAM. (bottom) Number of higher-amplitude transients per minute (continuous line) and the standard deviation (σ) of the RSAM (divided by 5, dashed line). The number of events was counted every 5 min. The average and standard deviation of the RSAM were calculated with a moving window with a duration and step of 5 and 3 min, respectively. Grey areas indicate example time periods with high σ and low events rate (area a), relatively high σ and high events rate (area b), and with low σ but high events rate (area c). This example is from 7 January 2005 (two examples of tremor waveform and their spectra in Figure 11).

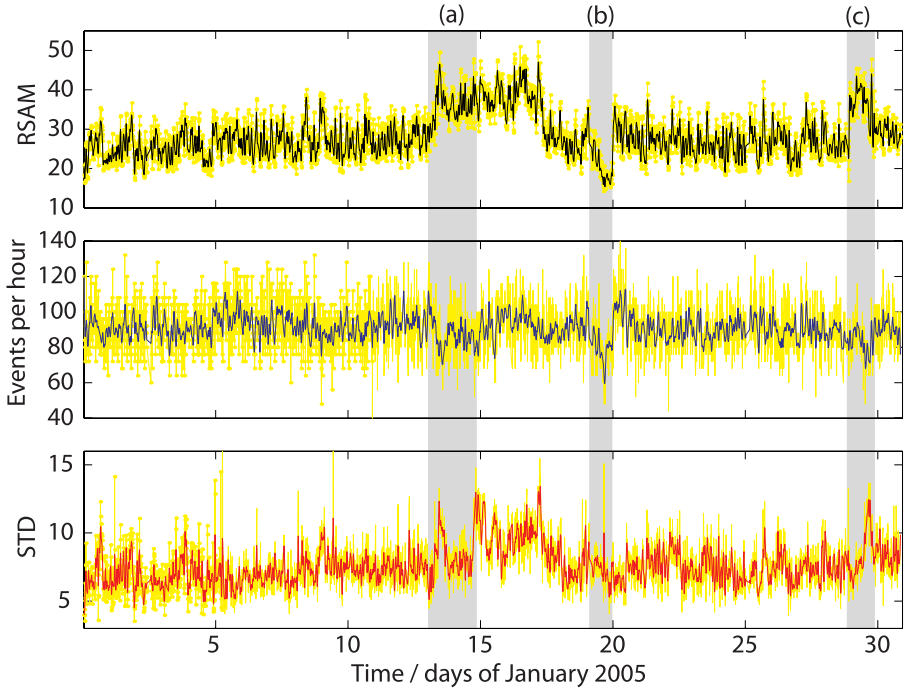

Figure 14. (top) RSAM amplitude, (middle) number of events per hour, and (bottom) RSAM standard deviation of the tremor signal in January 2005. The RSAM was calculated with a moving window with duration and step of 10 and 7.5 s, respectively. RSAM average and standard deviation were calculated in a 15 min long window moving with a step of 10 min. In each case, a moving average (four data points) was applied (dark line). Grey areas mark time periods with abrupt changes in RSAM amplitude, and coincide with areas marked in Figure 10.

Table 2. Monthly Volcano-Tectonic Earthquakes Detected at Villarrica Volcano

Month	Number of VT[a]
Dec 2004	2
Jan 2005	4
Feb 2005	2
Mar 2005	10
Apr 2005	36
May 2005	5
Jun 2005	5
Jul 2005	0

[a]VT, volcano-tectonic earthquakes.

of the volcanic system. To better constrain the evolution of such changes, however, an adequate seismic array is needed around Villarrica volcano.

6. Magma Degassing

6.1. SO_2 Flux Measurements

[39] Despite the persistent passive degassing exhibited for more than 20 years, measurements of gas composition and emission rates have not been done regularly at Villarrica volcano. *Witter et al.* [2004] and *Witter and Calder* [2004] contributed most of the data available on SO_2 fluxes and on the gas composition of the plume. They measured sulphur dioxide fluxes using ground-based correlation spectroscopy (COSPEC) in early 2000 and 2001. For this work, the new ultraviolet spectrometer (UVS) known as FLYSPEC [*Horton et al.*, 2006] was utilized. The hardware design of this UVS is based on fore optics, electronics, the USB2000 ultraviolet spectrometer from Ocean Optics, and a computer for recording and processing of the acquired spectra. See *Galle et al.* [2002], *Horton et al.* [2006], *Elias et al.* [2006], and *Edmonds et al.* [2003, and references therein] for more details on the design and capabilities of these instruments. The procedure for gas concentration retrieval is based on differential optical absorption spectroscopy (DOAS) [*Platt*, 1994], and has been described by *Horton et al.* [2006] and *Elias et al.* [2006]. Software designed specially for FLYSPEC allows the user to calibrate the instrument in the field and to get real-time SO_2 path length concentrations.

[40] In order to estimate the SO_2 flux from Villarrica volcano, ground-based traverses were carried out on the roads that surround the volcano, between 10 and 20 km away from the crater (Figure 1). These traverses were performed on 6 days between November 2004 and January 2005 and on 3 days in January–February 2006 (Table 3). Measurements on the southeast side of the volcano, that coincide with the direction of the prevailing winds, could not be completed owing to the unsuitable conditions of the road for traverses, and so those measurements were not included in this paper. The calibration of the FLYSPEC instrument was performed using a pair of calibration cells with concentrations 438 and 1504 ppm m and, on some occasions, was additionally complemented with calibration cells of 170 and 704 ppm m.

[41] The estimation of plume velocity is one of the primary sources of error in SO_2 flux measurements [*Stoiber et al.*, 1983]. For this work, the National Centers for Environmental Prediction (NCEP) Reanalysis data [*Kalnay et al.*, 1996], provided by NOAA-CIRES (Climate Diagnostics Center, Boulder, Colorado; available at http://www.cdc.noaa.gov/), were used for wind velocity estimates. These estimates are generated by using a state-of-the-art analysis system to perform data assimilation using past data from numerical models as well as from direct observations of atmospheric conditions [*Kalnay et al.*, 1996]. Comparison of our observations of plume dispersion and wind direction obtained from the NCEP Reanalysis data show very good agreement. At Villarrica volcano, a few estimations of plume speed were performed observing at the plume up to 5 km away from the crater. The comparison of these estimates with the interpolated wind field extracted from the NCEP Reanalysis data yielded differences of less than 50% in wind speed. However, it is not possible to accurately quantify the error using this method. Therefore,

Table 3. Summary of the Results of Ground-Based Traverses Carried Out to Estimate SO_2 Emissions at Villarrica Volcano, Along With RSAM Averages for the Same Periods[a]

	RSAM			SO_2 Flux			Number
Date	Min	Mean	Max	Min	Mean	Max	of Runs
February–March 2000[b]							
29 Jan	14.7	15.9	17.6		178		1
30 Jan	12.3	13.6	14.8	327	353	379	2
2 Feb	13.5	14.9	16.2	203	274	338	6
5 Feb	14.6	17.6	19.5	95	209	352	11
7 Feb	14.9	16.5	19.8		121		1
13 Feb	14.8	16.4	17.9	177	204	231	2
14 Feb	13.4	16.1	20.1	126	151	195	7
3 Mar	12.9	14	15.1	127	149	163	5
7 Mar	11.9	13.7	17.8		174		1
18 Mar	11.5	13.1	15.8	241	374	614	3
21 Mar	10	12.2	14.3	429	694	1115	8
April–June 2000[c]							
1 Apr	12.3	15.4	18.3	152	269	333	9
4 May	9.3	11.2	12.7	47	171	298	7
1 Jun	9	10.2	11.6		80		1
January–February 2001[b]							
15 Jan	12.2	17.3	22.8	87	118	176	8
25 Jan	20.9	24.6	30.3	257	441	961	6
28 Jan	22.2	24.7	28.6	324	564	705	7
2 Feb	24.5	28.9	30.5	565	732	939	7
February 2003[d]							
8 Feb		15.1		277	397	518	2
12 Feb		15.1		190	281	363	4
November 2004							
10 Nov	12.0	14.5	17.8	178	261	356	10
January 2005							
13 Jan	23.4	28.3	33.4	553	735	993	6
15 Jan	32.4	37.6	42.9	1176	1299	1482	4
17 Jan	36.5	40	44.6	706	951	1080	4
19 Jan	21.8	26.5	30	384	603	742	6
24 Jan	22.6	26.7	34.2	772	996	1164	4
January–February 2006							
17 Jan	6.2	6.8	7.5	78	122	154	8
9 Feb	8.3	9.2	10	233	262	343	6
13 Feb	9.6	11.2	12.5	86	149	232	4

[a]Emissions given in [Mg/d].
[b]Gas data from *Witter et al.* [2004]. They used a COSPEC.
[c]Gas data from *Witter and Calder* [2004]. They used a COSPEC.
[d]Gas data from *Mather et al.* [2004]. They used a miniDOAS. RSAM values from 12 November 2004.

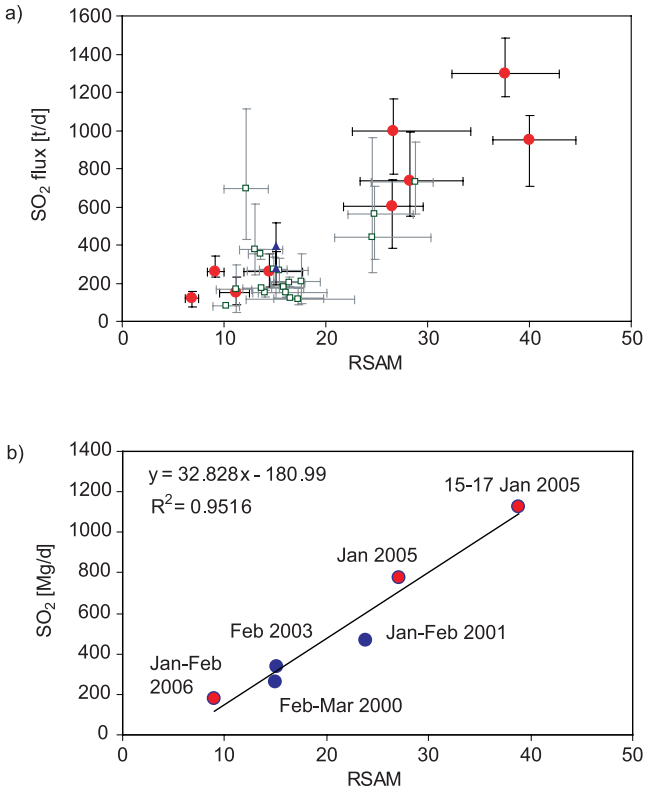

Figure 15. Correlation between RSAM and SO_2 flux observed at Villarrica volcano. (a) Daily averages; the vertical and horizontal bars show the minimum and maximum for individual traverses and hourly RSAM, respectively (Table 3). Squares are from *Witter et al.* [2004] and triangles are from *Mather et al.* [2004]. (b) Average seismic and gas data for different periods (of a few days to weeks) with available SO_2 flux measurements (Table 2).

for our results we maintain the overall error of 10–40% considered in previous studies that performed similar methodologies for SO_2 flux measurements [*Stoiber et al.*, 1983; *Kyle et al.*, 1994; *Williams-Jones et al.*, 2003; *Witter et al.*, 2004; *Rodríguez et al.*, 2004]. It is worth noting that, in any reported gas flux estimate lacking direct measurement of plume speed, this error can be much higher [*Rodríguez et al.*, 2004; *Williams-Jones et al.*, 2006].

6.2. Results and Correlation Between SO_2 Flux and RSAM

[42] Sulfur dioxide emitted from the crater of Villarrica volcano during November 2004 to January 2005, on individual traverses, ranged between 180 and 1500 metric tons per day (Mg/d) (Table 3 and Figure 15). Daily averages ranged between 260 and 1300 Mg/d; that is a fivefold difference. This range includes values that are clearly higher than those obtained in previous studies (in 2000–2001 and 2003 [*Witter et al.*, 2004; *Mather et al.*, 2004]). During the period January–February 2006 the gas fluxes were considerably lower, with daily averages no higher than 300 Mg/d. These new results highlight the variability of gas emissions at Villarrica volcano. Further, they were obtained at periods with different levels of activity, which contributes to a more representative analysis and correlation with seismicity and the observable activity of the lava lake. The highest SO_2 flux measured coincides with high levels of activity on 15–17 January 2005 and high values of RSAM. Conversely, the lowest fluxes were measured during periods of background (low) levels of volcanic activity: February–March 2000, February 2003, and January–February 2006 (Figure 15). For comparison, considering SO_2 emission rates of 200–500 Mg/d as representative of background levels of volcanic activity, degassing at Villarrica is lower compared to similar open vent systems such as Masaya (350–1800 Mg/d [*Duffell et al.*, 2003]), Stromboli (300–1200 Mg/d [*Allard et al.*, 1994]), Yasur (216–1665 Mg/d [*Bani and Lardy*, 2007]), and Pacaya (350–2400 Mg/d [*Rodríguez et al.*, 2004]), and higher than Erebus (16–71 (up to 230) Mg/d [*Kyle et al.*, 1994]). (*Andres and Kasgnoc* [1998] reported time-averaged values of 790, 730, 900, 510, and 79 Mg/d for Masaya, Stromboli, Yasur, Pacaya and Erebus, respectively.) It is noteworthy that the total emission of sulfur dioxide is subject to the variations in SO_2 fluxes that these volcanoes can manifest during periods with different levels of activity. For instance, at Yasur and Villarrica the emission of sulfur dioxide can exhibit more than a fivefold increase between low- and high-activity phases.

[43] Measured SO_2 emission rates of individual traverses exhibit a high variability on any particular day (Table 3). These fluctuations are the consequence of the combination of four phenomena: (1) the unsteady emission from the lava lake, in part owing to the concurrence of "passive" and explosive outgassing, (2) accumulation of gas between the magma free surface and the spatter roof, (3) the gas plume-air turbulent mixing and circulation caused by the combination of the rise of the thermal plume and wind velocity fluctuations inside the crater, and (4) nonuniform dispersion of the gas plume between the crater and the location where it is measured. In addition, a single traverse spans a time period in which the transport and dispersion of the gas plume continues and, therefore, the final gas column abundance profile measured might not be representative of the actual plume cross section at a specific time. All these variables contribute to the scattered results of daily SO_2 flux measurements.

[44] SO_2 flux data acquired herein (2004–2006) complemented by available measurements from previous studies (*Witter et al.* [2004] and *Witter and Calder* [2004] in 2000–2001; *Mather et al.* [2004] in 2003) show a good positive correlation with seismic amplitude (RSAM) (Table 3 and Figure 15). Similar to gas flux measurements, the 1-h-averaged RSAM (calculated from 0900 to 2100 LT) exhibits daily fluctuations. These variations in seismic amplitude are explained by the occurrence of banded tremor and changes in the frequency, length and amplitude of the higher-amplitude seismic transients. In particular, on days when the volcano showed elevated levels of activity (e.g., 13, 15, 17 January 2005), recognized by visual observations and high RSAM values, the emission of SO_2 was consistently higher (Figure 15a). This relation establishes a strong link between the generation of seismic tremor and outgassing activity. Similar correlations between SO_2 emissions and seismic amplitude have been found at

Table 4. Time-Averaged SO_2 Emissions at Villarrica Volcano Alongside RSAM Averages for Selected Periods and the Number of Days Over Which the Average Was Made[a]

Period	RSAM	SO_2	Number of Days
Feb–Mar 2000	14.9	263	12
Jan–Feb 2001	23.9	464	4
Feb 2003	15.1	339	2
Jan 2005	27.1	778	3
15–17 Jan 2005	38.8	1125	2
Jan–Feb 2006	9.1	178	3

[a]Emissions given in [Mg/d].

Mount Etna [*Leonardi et al.*, 2000] and Yasur [*Bani and Lardy*, 2007] volcanoes.

[45] Selected time periods in which Villarrica volcano exhibited sustained levels of activity allowed a better correlation between degassing and seismicity (Figure 15b and Table 4). During these periods, the activity observed at the crater remained unchanging along with the RSAM values. Assuming a uniform emission of SO_2 for each one of these periods, the average of daily results improves the precision of the measurements. Hence, a linear relationship SO_2 flux RSAM is obtained (Figure 15b):

$$SO_2[\mathrm{Mg/d}] = 32.8\ \mathrm{RSAM} - 181 \quad (1)$$

The negative value of the ordinate intercept (second value on the right hand side) of this linear equation implies a lateral displacement of the regression line to the right, meaning an abscissa intercept (at SO_2 = 0 Mg/d) of 5.5 RSAM units. Even though this value represents very low levels of volcano seismicity, it is within 30% of the RSAM values measured during background activity. Some plausible explanations for this displacement are that (1) tremor is not only caused by outgassing activity but also by another volcano-related or nonvolcanic phenomenon, (2) toward very low levels of outgassing and tremor magnitude the relationship turns nonlinear and the curve goes through the origin, or (3) this relationship is nonlinear but there is not enough data (or it is not accurate enough) to define it. As a first approximation, this relationship certainly serves as an estimation of the gas emitted from Villarrica volcano based on measurements of tremor magnitude.

7. Discussion

7.1. Volcanic Activity and Crater Morphology

[46] Currently, the interior of the crater is characterized by a spatter roof built above the surface of the lava lake, which constitutes the bottom of the crater. The descriptions presented herein illustrate how the depth and morphology of the spatter roof in the crater of the volcano change according to the degree of volcanic activity. Elevated or increasing activity levels are characterized by scoria terraces, spatter cones or pahoehoe lavas flooding the crater. The roof itself is very unstable and can experience major changes in morphology on a time span of hours to days. Low levels (or decreasing levels) of volcanic activity are commonly linked to a partly or totally collapsed roof, deep crater floor (perhaps with no roof), or a deep funnel shaped crater with no magmatic activity directly visible from the crater rim. The latter case implies that the top of the magma column is more than 100–150 m deep below the crater rim. Hence, the position, morphology and texture of the roof can give important information regarding changes in the depth of the magma column, and the intensity and type of activity taking place during the previous few days to weeks.

[47] The visibility of the lava lake is not directly related to the level of activity but instead to the depth of the lava free surface, morphology of the spatter roof, and the occurrence of roof collapses. Although strong explosions can affect the stability of the overlying roof, visual observations suggest a poor correlation between its collapses and the magnitude of explosions. However, the morphology of the spatter roof does have an effect on the apparent magnitude of explosions: they look stronger when the opening is big, by allowing pyroclastic material to be ejected freely out of the vent. Explosions also look stronger when a narrow cone-shaped vent is built on top of the spatter roof during elevated levels of activity, probably owing to the high level of the lava lake.

[48] The persistence and variability in outgassing styles observed at the lava lake is also evidenced by infrasound recording [*Johnson et al.*, 2004]. At Villarrica, the infrasound trace shows continuous pressure oscillations, including impulsive transients and small amplitude waveforms that repeat along the whole time series [see *Johnson et al.*, 2004, Figure 3]. The continuous bubble bursting activity observed at the surface of the lava lake reflects the highly dynamic convection of magma developed at shallow depths in the conduit. Convection of magma at the lava lake, as observed during the persistent seething magma activity, inhibits the development of a continuous crust over the lake surface. This convection is caused by the density difference between the hot and relatively gas-rich magma rising from deep levels in the magma column (or magma chamber), and the degassed and cooler magma that has reached the uppermost part of the system, which must sink back owing to its higher density [*Kazahaya et al.*, 1994; *Stevenson and Blake*, 1998]. In addition, the intensity of the convection is enhanced by the growing bubbles that form above gas supersaturation levels, by displacing the degassed melt sideways and downward as they pass upward. Hence, near the surface the convection is governed by bubbly to churn-type flow regime whose strength is dependent on the ascending gas flux [*Mudde*, 2005; *Xu et al.*, 1999]. We are not aware of this very dynamic flow regime, as represented by seething magma and small lava fountains, having been observed elsewhere. The continual arrival of bubbles to the surface observed during seething magma activity, with Strombolian explosions and small lava fountains taking place intermittently, suggest that bubbles ascend freely within the conduit. Coalescence of bubbles at the top of a reservoir before entering in to the upper conduit is unlikely to occur at Villarrica. Considering the conical shape and elevation of the volcanic edifice, approximately 2000 m, we suggest that the upper plumbing system of Villarrica volcano consists of a near-vertical conduit of cylindrical shape, with a length greater than 2000 m.

7.2. Relationship Between Outgassing and Seismicity

[49] Although we have no geophysical data appropriate to study the seismic source of the tremor, we have presented evidence that supports the relationship between the seismic-

ity and volcanic activity observed at the crater: (1) the tight correlation between visual observations of bursting events and rapid changes in tremor amplitude (transient events) (Figure 12a), (2) the predominance of low frequencies within the tremor (Figures 8 and 10), (3) the consistent frequency content of the low- and higher-amplitude tremor (Figure 12b), and (4) the positive correlation between RSAM and SO_2 flux (Table 3 and Figure 15).

[50] Much work carried out at other basaltic open vent volcanoes supports the link between tremor and outgassing activity [*Ripepe et al.*, 1996; *McGreger and Lees*, 2004; *Ripepe et al.*, 2001; *Métaxian et al.*, 1997; *Ripepe*, 1996; *Ripepe et al.*, 2002]. For instance, by using small aperture seismic arrays, *Métaxian et al.* [1997] analyzed the wavefield of the tremor at Masaya volcano. At the time of their study, lava lake activity was characterized by minor fountaining and audible outgassing. They concluded that the source of the tremor was seismic surface waves linked to superficial magmatic activity in Santiago crater. *Ripepe et al.* [2001] combined infrasound and seismicity to study a phase of vigorous Strombolian activity at Mount Etna, and concluded that the tremor was generated by a superposition of small point sources, lasting 1–2 s, due to pressure flux instability induced by magma degassing in the shallow portion of the magma column. At Stromboli, combination of seismicity with infrasound and thermal recording has demonstrated that the source of tremor resides in the explosive outgassing activity [*Ripepe et al.*, 1996; *Ripepe and Gordeev*, 1999; *Ripepe et al.*, 2002].

[51] The results presented herein on the activity of Villarrica volcano yield complementary insights into the results obtained from the analysis of tremor source at similar open vent volcanoes. We suggest that the tremor at Villarrica volcano, in particular the higher-amplitude transients, is produced by seismic surface waves resulting from gas ascent and outgassing activity taking place at the top of the magma column.

7.3. Relationship Between Bubble Bursting Styles

[52] A schematic diagram of the relationship between different explosive outgassing events observed at Villarrica is proposed on the basis of their duration and strength (Figure 16). (Here, the strength of the bubble bursting activity is estimated as the height above the surface of the lava lake that pyroclastic material can reach, which is related to the mass fraction of volatiles, overpressure and magma rise velocity [*Wilson*, 1980].) This diagram is qualitative and is intended to clarify the identification of new styles of bubble burst events described herein that, in a general sense, have been described in previous work as "Strombolian activity" [*Ortiz et al.*, 2003; *Witter et al.*, 2004].

[53] At one end, seething magma is considered the activity with the longest duration and low strength. Although its duration has not been constrained, on the basis of direct visual observations of the lava lake it is believed that this activity is continuous in time but with fluctuations in strength: from mild seething magma, whose lower end corresponds to gently rollover of the lava surface, to vigorous seething magma, whose upper end is lava fountaining. Seething magma has been observed to evolve into a small lava fountain in a time span of a few seconds (see

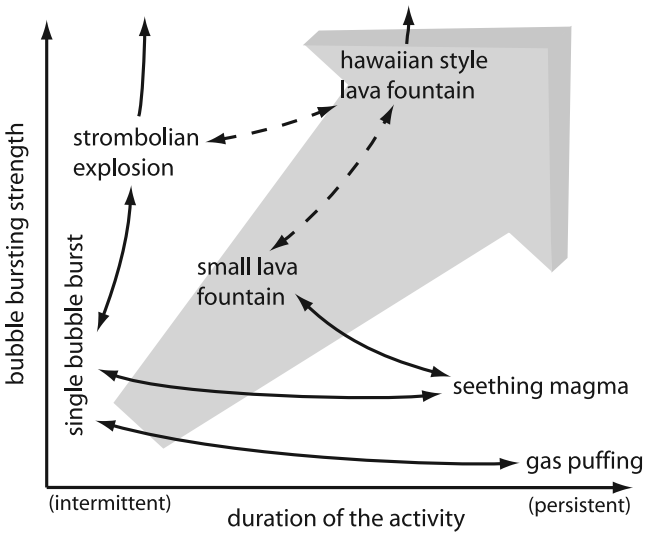

Figure 16. Schematic diagram of bubble burst styles that shows the relationship between the duration and strength of the events. Continuous line connections denote the continuum between events, whereas dashed line connections denote the feasible occurrence, although not observed directly at Villarrica, of a continuum between Strombolian explosions or small lava fountains, and the Hawaiian-style fountaining. The grey arrow denotes the increase in total gas emission as the duration and strength of the events increases.

Animations S1–S3 in the auxiliary material). Occasionally, the activity falls in between the two extremes, appearing as a vigorous seething magma or as a very small lava fountain (Figure 16). The occurrence of the small lava fountain activity at or near the surface of the lava lake, involving a higher amount of bubbles bursts than seething magma, indicates higher gas contents rising in packets at slightly higher velocities determined by the density of the melt-bubbles mixture. These fluctuations in gas (bubble) content in the vertical column of magma can be interpreted on the basis of waves of bubbles [*Manga*, 1996], in which bubbles ascending within the conduit tend to concentrate into layers (or clusters) owing to the decreasing rise speed of the bubbles as their concentration increases. Consequently, gas bubbles reach the surface in packets rather than with an uniform vertical distribution. A similar mechanism has been invoked to explain gas puffing activity at Stromboli volcano [*Ripepe et al.*, 2002]. The persistent gas puffing activity, characteristic of Stromboli volcano [*Ripepe et al.*, 2002; *Harris and Ripepe*, 2007b], is also included in the sketch of Figure 16.

[54] At the other extreme, Strombolian explosions are relatively short and display a broad range of behavior, from relatively mild single bubble bursts to major explosions that can send pyroclastic material hundreds of meters above the lava lake. The link between Strombolian explosions and seething magma is not a continuum. Strombolian explosions are considered isolated events that interrupt the seething magma activity.

[55] Although Hawaiian style lava fountaining is not part of the common activity seen during periods of volcanic

quiescence, in which the lava is confined inside the crater, it is included in Figure 16 to map the relation with respect to the other types of primary bubble burst seen at Villarrica. For instance, Strombolian explosions with very high bursting frequency can look similar to a Hawaiian style lava fountain [e.g., *Chester et al.*, 1985, pp. 126–130]. *Parfitt and Wilson* [1995] stated that it is the combination of the rise speed of the magma and the degree of bubble coalescence that defines the respective style of activity, where the magma gas content and viscosity influence only the conditions in which the transition between these two styles occurs. Hawaiian-style lava fountaining requires a relatively high magma rise speed and little coalescence of bubbles, which cause a highly vesicular melt that disrupts at deep levels (high pressure), whereas Strombolian explosions are caused by a slow rise of the magma in which coalescence plays a fundamental role in the generation of large bubbles that disrupt the magma at the magma-atmosphere surface. A twofold change in magma rise speed might be sufficient for the transition between one style of activity to the other [*Parfitt and Wilson*, 1995]. Changes in the physical properties of magma are plausible within the open system of Villarrica volcano. They can be a consequence of either entry of new gas-rich batches of magma into the system, or heterogeneous magma distribution and convection in a magma chamber, that could eventually vary the properties of the magma rising into the upper plumbing system. Hence, entry of magma with higher gas content and lower density into the system will exhibit a higher rise speed and, consequently, increase the gas flow rate within the upper part of the conduit. Depending on the extent of these changes, the outgassing activity can evolve from seething magma to lava fountaining of specific height and extrusion rate.

7.4. Volcano Monitoring

[56] Seismic tremor is the most common and continuous type of seismicity related to the activity of Villarrica volcano. Its amplitude, evaluated as RSAM units, has been shown to correlate well with the level of the activity observed at the summit. For instance, the different features shown in Figure 8 between January and April 2005 correlate with the increase in activity and evolution of the spatter roof (Table 1). Changes in seismic amplitude were also part of the elevated activity of 1999 [*Calder et al.*, 2004], as well as of the rapid changes in the level of the magma column observed at the end of 2000 [*Ortiz et al.*, 2003].

[57] The abnormal sequence of events that took place in 2000 [*Ortiz et al.*, 2003] is an example of variations in the type of volcanic activity accompanied by clear changes in the frequency distribution of the seismicity. These results and our analysis of the activity during November 2004 to April 2005 show that the amplitude and frequency distribution of the tremor can be good indicators of the variations in the activity of Villarrica volcano. However, during this time the relationship between the variations in frequency content and type or evolution of the volcanic activity was not straightforward. We hypothesize that elevated high frequencies (2.15–5.5 Hz) are caused by a rise in the level of the lava lake, perhaps interacting strongly with the spatter roof. Support for this idea comes from the positive correlation between gas flux and seismic amplitude that is in accordance with stronger levels of degassing, and therefore, with vertical expansion of the magma column. Moreover, during one of the periods that exhibit high frequencies, 15–19 January, instability and collapse of the roof was directly observed.

[58] Volcano-tectonic (VT) earthquakes are uncommon in the background seismicity at Villarrica volcano. VT-type seismicity is the result of rock failure caused by an increase in pressure within the magmatic system that is transferred to the country rock [*McNutt*, 2005]. Such a pressure increase can occur owing to new inputs of magma into the system and/or increasing degassing. The eruption in 1971, which involved the opening of a fracture in the upper part of the edifice and the generation of fissure-fed lava flows, is an example of this pressure rise and subsequent magma intrusion. If this fracturing occurs at deeper levels, it can lead to emplacement of magma as dikes or sills, which may reach the surface and initiate a flank eruption. Furthermore, because of the open state of the system, the occurrence of a shallow magma intrusion or increasing degassing will be accompanied by variations in the activity observed at the summit. The elevated SO_2 flux measured during January and the appearance of VT earthquakes during March–April 2005, were strong evidence of an increase in the pressure of the system related to stronger degassing, perhaps caused by the supply of volatile-rich magma. It is not possible to know, however, how close the volcano was from starting a renewed eruptive episode. This anomalous episode did not last for long, as the VT earthquakes vanished in June and toward the end of July the activity at the crater declined to background levels (Table 4).

[59] In addition to seismic characteristics, visual observations of the activity in the crater give valuable information regarding the level of the magma column and its variations, as well as the style of activity taking place. Some important parameters worth considering are (1) the position and morphology of the spatter roof, (2) the texture of its surface, (3) presence and texture of new material on the crater rim, (4) frequency of the big explosions, and (5) the height above the crater floor that ejected pyroclasts can reach. Furthermore, continual measurements of SO_2 fluxes would be a significant contribution to the monitoring of degassing levels at Villarrica. The correlation of these gas data with seismicity and visual observations of activity in the crater offer a fuller appreciation of the current state and variations of the volcanic activity, and help to understand the evolution of the magmatic system.

8. Conclusions

[60] Villarrica is a basaltic to basaltic andesite open vent stratovolcano with a very active lava lake and persistent gas emission. Three primary styles of bubble bursting have been recognized at the magma free surface: seething magma, small lava fountains, and Strombolian explosions. Seething magma is a distinctive activity of Villarrica volcano, which may contrast to the activity observed at other open vent volcanoes, and involves the continuous arrival and bursting of gas bubbles with radii generally lower than 5 m. Strombolian explosions can be variable in duration, from a single bubble burst (although rare) to a bursting sequence (>15 s) derived from the ascent of major gas slugs. Small

lava fountains are intermediate (in style, length and strength of the bursting event) between seething magma and Strombolian explosions. Long-duration lava fountains (>30 s) must result from large gas pockets that reach the surface of the lava lake. The interaction of bubble bursting activity with the spatter roof can be manifested by two other types of events: gas jetting and "splashing" magma. The strength and style of the outgassing activity are associated with variations in the height of the magma column, leaving an imprint in the position, morphology and texture of the spatter roof.

[61] The activity at the crater of Villarrica volcano shows fluctuations on the scale of months to years. Slow increase in the activity at Villarrica, as observed during November 2004 and May 2005, exhibited a rise in the magma column reflected in the position of the spatter roof (at least 60 m), higher SO_2 fluxes (we measured up to 1500 t/d), and an increase in the frequency and strength of Strombolian explosions. This evolution was also evidenced in the higher tremor amplitude as well as the presence of VT earthquakes. Hence, typical background (low) levels of activity correspond to a lava lake located >80 m below the crater rim, small and/or blocky morphology of the roof, seismic amplitude (RSAM) lower than 25 units, few VT earthquakes, and daily averages of SO_2 emissions lower than 600 t/d. Elevated levels of activity show fluctuations in the height of the magma column, changes in the morphology of the spatter roof, and changes in the characteristics of the bubble bursting activity. Available SO_2 flux data also suggest an increase in gas emission rates during periods of elevated activity.

Appendix A: Details of the Calculation of the Tremor Statistics

[62] The real time seismic amplitude (RSAM) is calculated over the whole time series by means of a moving average window in the time domain. For a particular time, t, the RSAM is calculated as follows:

$$\mathrm{RSAM}(t) = \frac{1}{T}\sum_{l=t-\frac{T}{2}}^{t+\frac{T}{2}} |s(l)| \qquad \text{(A1)}$$

where T is the duration of the moving time window and $|s(t)|$ corresponds to the absolute value of the seismic signal. The length of the resulting RSAM time series depends on the overlap (or time step) of the moving window. The selection of both the duration (T) and time step determines the resolution of the RSAM and affects the results and meaning of the analysis. In particular, it is desirable to be able to identify each of the higher-amplitude transients (or events) of the tremor, thereby the rate of events can be calculated. Accordingly, values of 10 and 7.5 s (25% overlap) for the duration of the window and time step, respectively, have been found appropriate for the statistical analysis of tremor amplitude at Villarrica volcano (Figures 13–14).

[63] Once the RSAM(t) has been obtained, another moving window is applied over the RSAM time series in which the mean ($\overline{\mathrm{RSAM}}$) and standard deviation (σ) are calculated. The duration (ΔT) and time step (δt) of this window are dependent on the objective of the analysis. For instance, the study of the characteristics and waveform of the tremor, as well as the hourly fluctuations in its amplitude, were carried out using ΔT = 300 s and δt = 180 s (Figure 13). To study long-term variations, ΔT = 900 s and δt = 600 s were chosen (Figure 14).

[64] A third parameter, the rate of higher-amplitude events, was calculated by counting the amount of these events over a time window of duration equivalent to ΔT. An event corresponds to a peak in the RSAM time series whose magnitude is above the average ($\overline{\mathrm{RSAM}}$) calculated for that window. To identify the peaks, a forward finite difference was performed beforehand in the RSAM time series that was used to find those elements of the series with a preceding positive derivative and followed by a negative derivative.

[65] **Acknowledgments.** We acknowledge the Southern Chile Volcano Observatory (OVDAS–SERNAGEOMIN) for their support and seismic data. Keith Horton is thanked for helping with the setting up of the FLYSPEC instrument and assistance with the software for processing of the spectral data. We thank Chris Newhall and Darcy Ogden for their useful reviews of the paper. E. S. C. was funded by a Royal Society Dorothy Hodgkin Fellowship. In addition, both J. L. P. and E. S. C. were funded by an Open University career development grant.

References

Adams, N. K., B. F. Houghton, and W. Hildreth (2006), Abrupt transitions during sustained explosive eruptions: Examples from the 1912 eruption of Novarupta, Alaska, *Bull. Volcanol.*, *69*, 189–206.

Allard, P., J. Carbonnelle, N. Mètrich, H. Loyer, and P. Zettwoog (1994), Sulphur output and magma degassing budget of Stromboli volcano, *Nature*, *368*, 326–329.

Andres, R., and A. Kasgnoc (1998), A time-averaged inventory of subaerial volcanic sulfur emissions, *J. Geophys. Res.*, *103*(D19), 22,251–25,261.

Andronico, D., et al. (2005), A multi-disciplinary study of the 2002–03 Etna eruption: Insights into a complex plumbing system, *Bull. Volcanol.*, *67*, 314–330.

Aster, R., S. Mah, P. Kyle, W. McIntosh, N. Dunbar, J. Johnson, M. Ruiz, and S. McNamara (2003), Very long period oscillations of Mount Erebus volcano, *J. Geophys. Res.*, *108*(B11), 2522, doi:10.1029/2002JB002101.

Bani, P., and M. Lardy (2007), Sulphur dioxide emission rates from Yasur volcano, Vanuatu archipelago, *Geophys. Res. Lett.*, *34*, L20309, doi:10.1029/2007GL030411.

Bertagnini, A., N. Métrich, P. Landi, and M. Rosi (2003), Stromboli volcano (Aeolian Archipelago, Italy): An open window on the deep-feeding system of a steady state basaltic volcano, *J. Geophys. Res.*, *108*(B7), 2336, doi:10.1029/2002JB002146.

Bluth, G., J. M. Shannon, I. Watson, A. Prata, and V. Realmuto (2007), Development of an ultra-violet digital camera for volcanic SO_2 imaging, *J. Volcanol. Geotherm. Res.*, *161*, 47–56.

Bohm, M., S. Luth, H. Echtler, G. Asch, K. Bataille, C. Bruhn, A. Rietbrock, and P. Wigger (2002), The southern Andes between 36° and 40°S latitude: Seismicity and average seismic velocities, *Tectonophysics*, *356*, 275–289, doi:10.1016/S0040-1951(02)00399-2.

Calder, E., A. Harris, P. Peña, E. Pilger, L. Flynn, G. Fuentealba, and H. Moreno (2004), Combined thermal and seismic analysis of the Villarrica volcano lava lake, Chile, *Rev. Geol. Chile*, *31*(2), 259–272.

Calvari, S., L. Spampinato, and L. Lodato (2006), The 5 April 2003 vulcanian paroxysmal explosion at Stromboli volcano (Italy) from field observations and thermal data, *J. Volcanol. Geotherm. Res.*, *149*(1–2), 160–175.

Casertano, L. (1963), Activity of Villarrica volcano in the current century (in Spanish), *Bol. Univ. Chile*, *40*, 22–28, 48–54.

Chester, D., A. Duncan, J. Guest, and C. Kilburn (Eds.) (1985), *Mount Etna: The Anatomy of a Volcano*, Stanford Univ. Press, Stanford, Calif.

Clavero, J., and H. Moreno (2004), Evolution of Villarrica volcano, in *Villarrica Volcano (39.5°S), Southern Andes, Chile*, Bol. 61, pp. 17–27, edited by L. E. Lara and J. Clavero, Serv. Nac. de Geol. y Miner., Santiago, Chile.

Duffell, H. J., C. Oppenheimer, D. M. Pyle, B. Galle, A. J. McGonigle, and M. R. Burton (2003), Changes in gas composition prior to a minor explosive eruption at Masaya volcano, Nicaragua, *J. Volcanol. Geotherm. Res.*, *126*, 229–327.

Edmonds, M., R. Herd, B. Galle, and C. Oppenheimer (2003), Automatic, high time-resolution measurements of SO_2 flux at Soufriére Hills volcano, Montserrat, *Bull. Volcanol.*, *65*, 578–586.

Elias, T., A. J. Sutton, C. Oppenheimer, K. A. Horton, H. Garbeil, V. Tsanev, A. J. S. McGonigle, and G. Williams-Jones (2006), Comparison of COSPEC and two miniature ultraviolet spectrometer systems for SO_2 measurements using scattered sunlight, *Bull. Volcanol.*, *68*, 313–322.

Endo, T., and T. Murray (1991), Real-time seismic amplitude measurement (RSAM): A volcano monitoring and prediction tool, *Bull. Volcanol.*, *53*, 533–545.

Falsaperla, S., S. Alparone, S. D'Amico, G. Granzia, F. Ferrari, H. Langer, T. Sgroi, and S. Spampinato (2005), Volcanic tremor at Mt. Etna, Italy, preceding and accompanying the eruption of July–August, 2001, *Pure Appl. Geophys.*, *162*, 2111–2132.

Fischer, T. P., K. Roggensack, and P. R. Kyle (2002), Open and almost shut case for explosive eruptions: Vent processes determined by SO_2 emission rates at Karymsky Volcano, Kamchatka, *Geology*, *30*(12), 1059–1062.

Fuentealba, G., and P. Peña (1998), Instalación y puesta en funcionamiento del sistema de monitoreo sismológico del volcán Villarrica, durante el primer semestre de 1998, report, 13 pp., Serv. Nac. de Geol. y Miner., Santiago, Chile.

Fuentealba, G., P. Peña, and E. Calder (2000), Sustained tremor, open system degassing and annual perturbations at the Villarrica volcano lava lake, Chile, paper presented at IX Congreso Geológico Chileno, Geol. Soc. of Chile, Puerto Varas, Chile.

Galle, B., C. Oppenheimer, A. Geyer, A. McGonigle, M. Edmonds, and L. Horrocks (2002), A miniaturised ultraviolet spectrometer for remote sensing of SO_2 fluxes: A new tool for volcano surveillance, *J. Volcanol. Geotherm. Res.*, *119*(1), 241–254.

Gerlach, T. M. (1986), Exsolution of H_2O, CO_2, and S during eruptive episodes at Kilauea volcano, Hawaii, *J. Geophys. Res.*, *91*, 12,177–12,185.

Harris, A., and M. Ripepe (2007a), Synergy of multiple geophysical approaches to unravel explosive eruption conduit and source dynamics—A case study from Stromboli, *Chemie Erde Geochem.*, *67*, 1–35.

Harris, A., and M. Ripepe (2007b), Temperature and dynamics of degassing at Stromboli, *J. Geophys. Res.*, *112*, B03205, doi:10.1029/2006JB004393.

Harris, A. J., R. Carniel, and J. Jones (2005), Identification of variable convective regimes at Erta Ale lava lake, *J. Volcanol. Geotherm. Res.*, *142*, 207–223.

Hickey-Vargas, R., L. López-Escobar, H. Moreno, J. Clavero, L. Lara, and M. Sun (2004), Magmatic evolution of the villarrica volcano, in *Villarrica Volcano (39.5°S), Southern Andes, Chile*, Bol. 61, pp. 39–45, edited by L. E. Lara and J. Clavero, Serv. Nac. de Geol. y Miner., Santiago, Chile.

Horton, K., G. Williams-Jones, H. Garbeil, T. Elias, A. Sutton, P. Mouginis-Mark, J. Porter, and S. Clegg (2006), Real-time measurement of volcanic SO_2 emissions: Validation of a new UV correlation spectrometer (FLYSPEC), *Bull. Volcanol.*, *68*, 323–327.

Johnson, J. B., R. C. Aster, and P. R. Kyle (2004), Volcanic eruptions observed with infrasound, *Geophys. Res. Lett.*, *31*, L14604, doi:10.1029/2004GL020020.

Kalnay, E., et al. (1996), The NCEP/NCAR 40-year reanalysis project, *Bull. Am. Meteorol. Soc.*, *77*(3), 437–471.

Kazahaya, K., H. Shinohara, and G. Saito (1994), Excessive degassing of Izu-Oshima volcano: Magma convection in a conduit, *Bull. Volcanol.*, *56*, 207–216.

Koyanagi, R., B. Chouet, and K. Aki (1987), Origin of volcanic tremor in Hawaii, I, Compilation of seismic data from the Hawaiian Volcano Observatory, 1972 to 1985, *U.S. Geol. Surv. Prof. Pap.*, *1350*, 1221–1258.

Kyle, P., L. Sybeldon, W. McIntoch, K. Meeker, and D. R. Symonds (1994), Sulfur dioxide emission rates from Mount Erebus, Antartica, in *Volcanological and Environmental Studies of Mount Erebus, Antartica*, *Antarct. Res. Ser.*, vol. 66, edited by P. Kyle, pp. 69–82, AGU, Washington, D. C.

Lautze, N. C., and B. F. Houghton (2007), Linking variable explosion style and magma textures during 2002 at Stromboli volcano, Italy, *Bull. Volcanol.*, *69*, 445–460.

Lavenu, A., and J. Cembrano (1999), Compressional and transpressional-stress pattern for Pliocene and Quaternary brittle deformation in fore arc and intra-arc zones (Andes of central and southern Chile), *J. Struct. Geol.*, *21*, 1669–1691.

Leonardi, S., S. Gresta, and F. Mulargia (2000), Cross-correlation between volcanic tremor and SO_2: Flux data from Mount Etna volcano, 1987–1992, *Phys. Chem. Earth, Part A*, *25*(9–11), 737–740.

López-Escobar, L., J. Cembrano, and H. Moreno (1995), Geochemistry and tectonics of the Chilean southern Andes basaltic Quaternary volcanism (37°–46°S), *Rev. Geol. Chile*, *22*(2), 219–234.

Manga, M. (1996), Waves of bubbles in basaltic magmas and lavas, *J. Geophys. Res.*, *101*(B8), 17,457–17,465.

Mather, T. A., V. I. Tsanev, D. M. Pyle, A. J. S. McGonigle, C. Oppenheimer, and A. G. Allen (2004), Characterization and evolution of tropospheric plumes from Lascar and Villarrica volcanoes, Chile, *J. Geophys. Res.*, *109*, D21303, doi:10.1029/2004JD004934.

McGreger, A. D., and J. M. Lees (2004), Vent discrimination at Stromboli volcano, Italy, *J. Volcanol. Geotherm. Res.*, *137*, 169–185.

McNutt, S. (2000), Seismic monitoring, in *Encyclopedia of Volcanoes*, edited by H. Sigurdsson et al., pp. 1095–1119, Academic, San Diego, Calif.

McNutt, S. R. (2005), Volcanic seismology, *Annu. Rev. Earth Planet. Sci.*, *32*, 461–491.

Métaxian, J., P. Lesage, and J. Dorel (1997), Permanent tremor of Masaya volcano, Nicaragua: wave field analysis and source location, *J. Geophys. Res.*, *102*(B10), 22,529–22,545.

Moreno, H., J. Clavero, and L. Lara (1994), Explosive post-glacial activity of Villarrica volcano, southern Andes (39°25′S), paper presented at 7th Congreso Geológico Chileno, Univ. of Concepción, Concepcion, Chile.

Mudde, R. F. (2005), Gravity-driven bubbly flows, *Annu. Rev. Fluid Mech.*, *37*, 393–423.

Oppenheimer, C., and G. Yirgu (2002), Thermal imaging of an active lava lake: Erta ëAle volcano, Ethiopia, *Int. J. Remote Sens.*, *23*(22), 4777–4782.

Ortiz, R., H. Moreno, A. García, G. Fuentealba, M. Astiz, P. Peña, N. Sánchez, and M. Tárraga (2003), Villarrica volcano (Chile): Characteristics of the volcanic tremor and forecasting of small explosions by means of a material failure method, *J. Volcanol. Geotherm. Res.*, *128*, 247–259.

Parfitt, E. A. (2004), A discussion of the mechanisms of explosive basaltic eruptions, *J. Volcanol. Geotherm. Res.*, *134*(1–2), 77–107.

Parfitt, E. A., and L. Wilson (1995), Explosive volcanic eruptions—IX. The transition between Hawaiian-style lava fountaining and Strombolian explosive activity, *Geophys. J. Int.*, *121*, 226–232, doi:10.1111/j.1365-246X.1995.tb03523.x.

Patrick, M. R., A. J. L. Harris, M. Ripepe, J. Dehn, D. A. Rothery, and S. Calvari (2007), Strombolian explosive styles and source conditions: insights from thermal (FLIR) video, *Bull. Volcanol.*, *69*(7), 769–784.

Platt, U. (1994), Differential optical absorption spectroscopy (DOAS), in *Air Monitoring by Spectroscopic Techniques*, *Chem. Anal. Ser.*, vol. 127, edited by M. Sigrist, pp. 27–84, John Wiley, New York.

Ripepe, M. (1996), Evidence for gas influence on volcanic seismic signal recorded at Stromboli, *J. Volcanol. Geotherm. Res.*, *70*, 221–233.

Ripepe, M., and E. Gordeev (1999), Gas bubble dynamics model for shallow volcanic tremor at Stromboli, *J. Geophys. Res.*, *104*, 10,639–10,654.

Ripepe, M., P. Poggi, T. Braun, and E. Gordeev (1996), Infrasonic waves and volcanic tremor at Stromboli, *Geophys. Res. Lett.*, *23*(2), 181–184.

Ripepe, M., M. Coltelli, E. Privitera, S. Gresta, M. Moretti, and D. Piccinini (2001), Seismic and Infrasonic Evidences for an Impulsive Source of the Shallow Volcanic Tremor at Mt. Etna, Italy, *Geophys. Res. Lett.*, *28*(6), 1071–1074.

Ripepe, M., A. J. Harris, and R. Carniel (2002), Thermal, seismic and infrasonic evidences of variable degassing rates at Stromboli volcano, *J. Volcanol. Geotherm. Res.*, *118*, 285–297.

Ripepe, M., A. J. L. Harris, and E. Marchetti (2005), Coupled thermal oscillations in explosive activity at different craters of Stromboli volcano, *Geophys. Res. Lett.*, *32*, L17302, doi:10.1029/2005GL022711.

Rodríguez, L. A., I. M. Watson, W. I. Rose, Y. K. Branan, G. J. Bluth, G. Chigna, O. Matías, D. Escobar, S. A. Carn, and T. P. Fischer (2004), SO_2 emissions to the atmosphere from active volcanoes in Guatemala and El Salvador, 1999–2002, *J. Volcanol. Geotherm. Res.*, *138*, 325–344.

Rowe, C., R. Aster, P. Kyle, R. Dibble, and J. Schlue (2000), Seismic and acoustic observations at Mount Erebus Volcano, Ross Island, Antarctica, 1994–1998, *J. Volcanol. Geotherm. Res.*, *101*, 105–128.

Ryan, S. (1995), Quiescent outgassing of Mauna Loa volcano 1958–1994, in *Mauna Loa Revealed: Structure, Composition, History, and Hazards*, *Geophys. Monogr. Ser.*, vol. 92, edited by J. Rhodes and J. P. Lockwood, pp. 95–115, AGU, Washington, D. C.

Shinohara, H., and J. B. Witter (2005), Volcanic gases emitted during mild Strombolian activity of Villarrica volcano, Chile, *Geophys. Res. Lett.*, *32*, L20308, doi:10.1029/2005GL024131.

Sparks, R. (2003), Dynamics of magma degassing, in *Volcanic Degassing*, edited by C. Oppenheimer, D. Pyle, and J. Barclay, *Geol. Soc. Spec. Publ.*, *213*, 5–22.

Stevenson, D., and S. Blake (1998), Modelling the dynamics and thermodynamics of volcanic degassing, *Bull. Volcanol.*, *60*, 307–317.

Stoiber, R., L. Lawrence, J. Malinconico, and W. Stanley (1983), Use of the correlation spectrometer at volcanoes, in *Forecasting Volcanic Events*, edited by H. Tazieff and J. Sabroux, pp. 425–444, Elsevier, Amsterdam.

Vergniolle, S. (1996), Bubble size distribution in magma chambers and dynamics of basaltic eruptions, *Earth Planet. Sci. Lett.*, *140*, 269–279.

Vergniolle, S., and M. Mangan (2000), Hawaiian and Strombolian eruptions, in *Encyclopedia of Volcanoes*, edited by H. Sigurdsson et al., pp. 447–461, Academic, San Diego, Calif.

Williams-Jones, G., H. Rymer, and D. A. Rothery (2003), Gravity changes and passive SO_2 degassing at the Masaya caldera complex, Nicaragua, *J. Volcanol. Geotherm. Res.*, *123*, 137–160.

Williams-Jones, G., K. A. Horton, T. Elias, H. Garbeil, P. J. Mouginis, M. A. J. Sutton, and A. J. L. Harris (2006), Accurately measuring volcanic plume velocity with multiple UV spectrometers, *Bull. Volcanol.*, *68*, 328–332.

Wilson, L. (1980), Relationships between pressure, volatile content and ejecta velocity in three types of volcanic explosion, *J. Volcanol. Geotherm. Res.*, *8*, 297–313.

Witter, J. B., and E. S. Calder (2004), Magma degassing at Villarrica volcano, in *Villarrica Volcano (39.5°S), Southern Andes, Chile*, Bol. 61, pp. 46–52, edited by L. E. Lara and J. Clavero, Serv. Nac. de Geol. y Miner., Santiago, Chile.

Witter, J. B., V. C. Kress, P. Delmelle, and J. Stix (2004), Volatile degassing, petrology, and magma dynamics of the Villarrica Lava Lake, southern Chile, *J. Volcanol. Geotherm. Res.*, *134*, 303–337.

Xu, J., P. Cheng, and T. Zhao (1999), Gas-liquid two-phase flow regimes in rectangular channels with mini/micro gaps, *Int. J. Multiphase Flow*, *25*, 411–432.

Young, S., B. Voight, and H. Duffell (2003), Magma extrusion dynamics revealed by high-frequency gas monitoring at Soufriére Hills volcano, Montserrat, in *Volcanic Degassing*, edited by C. Oppenheimer, D. Pyle, and J. Barclay, *Geol. Soc. Spec. Publ.*, *213*, 219–230.

Zobin, V. (2003), *Introduction to Volcanic Seismology*, 1st ed., 290 pp., Elsevier, New York.

D. Basualto, Southern Andes Volcano Observatory, Servicio Nacional de Geología y Minería, Avenida Francisco Salazar 01145, Casilla 54-D, Temuco, Chile.

S. Blake and D. A. Rothery, Department of Earth and Environmental Sciences, Open University, Milton Keynes MK7 6AA, UK.

E. S. Calder, Department of Geology, State University of New York at Buffalo, 876 Natural Sciences Complex, Buffalo, NY 14260-3050, USA.

J. L. Palma, Department of Geological and Mining Engineering and Sciences, Michigan Technological University, 1400 Townsend Drive, Houghton, MI 49931, USA. (jose@mtu.edu)